DESIGN OF AN IMPLANTABLE ANTENNA FOR MICROWAVE HYPERTHERMIA

by

Aydın Uzun

A report submitted for EE492 senior design project class
in partial fulfillment of the requirements for the degree of
Bachelor of Science
(Department of Electrical and Electronics Engineering)
in Boğaziçi University

January 4th, 2020

Principal Investigator: Sema Dumanlı Oktar

ACKNOWLEDGMENTS

I would like to thank Prof. Sema Dumanlı Oktar for her understanding; and for giving me the opportunity to work on her project SlmpliFy-B (Smart Orthopaedic Hip Implant Fighting Antimicrobial Resistant Bacteria.

ABSTRACT

Technology today affects every single aspect of modern society. In fact, there is not an industry out there that has not been affected by the hi-tech revolution. Whether we are talking about transportation, communication, security, banking or healthcare, they all rely on technology in one way or another. But nowhere is this immense impact more apparent than in the field of medicine and healthcare. Technological advancements are revolutionizing the way healthcare is being delivered and are also a key factor driving the advances of surgical treatment. But we are still far from fighting against orthopedic implant infection without major intervention and revision surgery. Staphylococcus aureus and Staphylococcus epidermidis are the leading etiologic agents of orthopedic implant infection. Traditional antibiotic therapy will never be successful against these pathogens after the biofilm is formed. This property of bacteria is called antimicrobial resistance (AMR) and it is a major concern worldwide.

A hip implant can be equipped with sensors and microelectronics forming a wireless communication link between the implant and an on-body sensor. In this project an antenna taking action against implant infection before and during the biofilm formation through microwave hyperthermia will be designed.

TABLE OF CONTENTS

LIST OF FIGURES

LIST OF TABLES

CHAPTER 1

INTRODUCTION

The recent technological advancements are revolutionizing the way healthcare is being delivered and they are also a key factor driving the advances of surgical treatment. Joint replacement surgery (hip and knee replacement) is considered the most effective intervention for severe osteoarthritis and hip fractures, reducing pain and disability and restoring some patients to near normal function. [1] As a consequence, hip replacement surgery shows increasing trends in most OECD countries. On average, the rate of hip replacement increased by 30% between 2000 and 2015.[1] Revision burden can be seen as a rough measure of the success of hip replacement surgeries. In the USA the revision burden was 10.2% for hips between 2012 and 2015 [2], but revision surgery of the hip is expensive owing to the increased cost of pre-operative investigations, surgical implants and instrumentation. [3]

The six most common indications for revision after primary hip replacement (listed in order of frequency) are aseptic loosening, pain, adverse soft tissue reaction to particulate debris, dislocation, infection and peri-prosthetic fracture.[4] Especially performing the revision surgery for infection is riskier considering the instrumentation. Staphylococcus aureus and Staphylococcus epidermidis are the leading etiologic agents of orthopedic implant infection.[5] Traditional antibiotic therapy will never be successful against these pathogens after the biofilm is formed. [6] This property of bacteria is called antimicrobial resistance (AMR) and it is a major concern worldwide. The other modes of treatment will be needed to prevent biofilm formation in the first place.

A hip implant can be equipped with sensors and microelectronics forming a wireless communication link between the implant and an on-body sensor to collect continuous data or provide real-time feedback.[7] In this project it is aimed to design an antenna taking action against infection before and during the biofilm formation through microwave hyperthermia with the help of the feedback from the antenna which monitors its environment.

CHAPTER 2

METHODOLOGY AND ANALYSIS (EE 491)

2.1 Design of CBSA

After literature review it is decided to use a cavity-backed slot antenna, because the cavity backed slot antenna (CBSA), where the slot is backed with rectangular cavity, achieves unidirectional radiation and has advantages of low profile, light weight and ease of integration. [8] The CBSA can be fed by probe, metal waveguide, substrate integrated waveguide (SIW), and microstrip, but the microstrip-fed CBSA has simple structure and small size. [8]

2.1.a In vacuum

In this step a CBSA is designed to operate at 2.4 GHz. The industrial, scientific and medical (ISM) 2.40 GHz radio band is an allowed band for body area networks or medical applications. [9] The performance of designed antenna is judged by its return loss and radiation pattern.

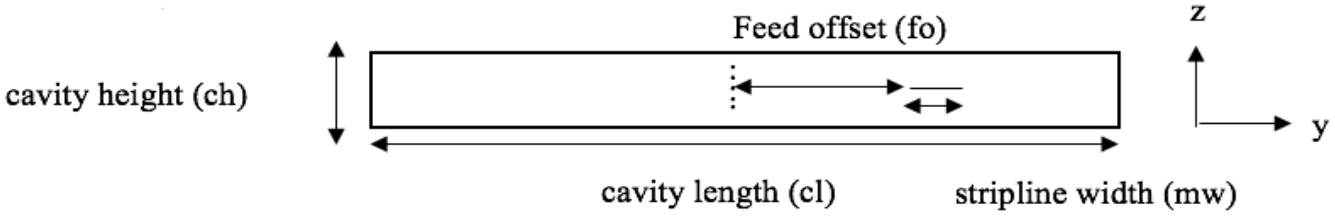

a) Modelled CBSA in yz plane

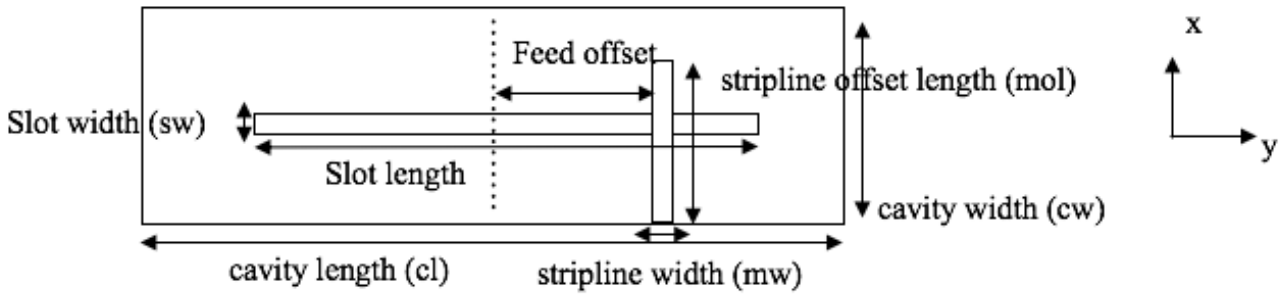

b) Modelled CBSA in xy plane

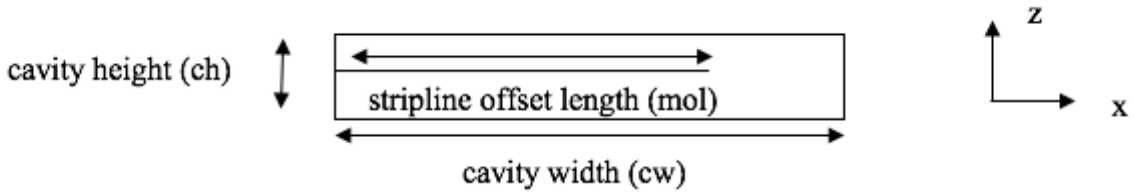

c) Modelled CBSA in xz plane

Figure 1: Modelled CBSA

The model of the designed antenna can be seen in Figure 1 from different perspectives. The dimensions of the model can be found in Table I.

The cavity is formed from a 3.15 mm thick (cavity height) substrate with a dielectric constant of 4.4 (FR-4). The slot is fed by a 50Ω stripline located in the vertical midplane of the antenna in z direction.

The initial dimensions other than the cavity height are determined using the HFSS Antenna Toolkit Software. Prior to the start of the optimization, the software introduces a microstrip feed slot antenna with the initial values of Table I, but this is not the desired antenna. After some modifications, the desired antenna is achieved, the model of which is shown in Figure 1.

The CBSA has been optimized for operation at 2.4 GHz with -20dB return loss. The optimization is done using software ANSYS Electromagnetics Suite. The dimensions given in Table I are parametrized and optimized for a return loss -20dB.

One conclusion that can be drawn from the optimization process is that the most critical parameters for matching are the parameters for the width of the stripline and the length of the stripline. In addition, sloth length is the most critical parameter in terms of CBSA resonance frequency.

The return loss curve of the optimized antenna can be seen in Figure 2.

Table I. Parametrized dimensions of CBSA in vacuum

Dimension	Initial value	Final value
Slot length	5.56 cm	5.2 cm
Slot width	0.28 cm	0.21 cm
Feed Offset	1.55 cm	1.8 cm
Stripline width	0.31 cm	0.15 cm
Stripline offset length	1.71 cm	0.53 cm
Cavity length	11.1 cm	8.1 cm
Cavity width	8.3 cm	3.2 cm

2.1.a In fat

The same procedure is used as in vacuum. The initial values of parametrized dimensions of the antenna optimized in fat are the final values of the antenna optimized in vacuum. It is obvious that the dimensions should change significantly to cause a return loss of -20dB, since

Figure 2: Simulated S_{11} vs Frequency

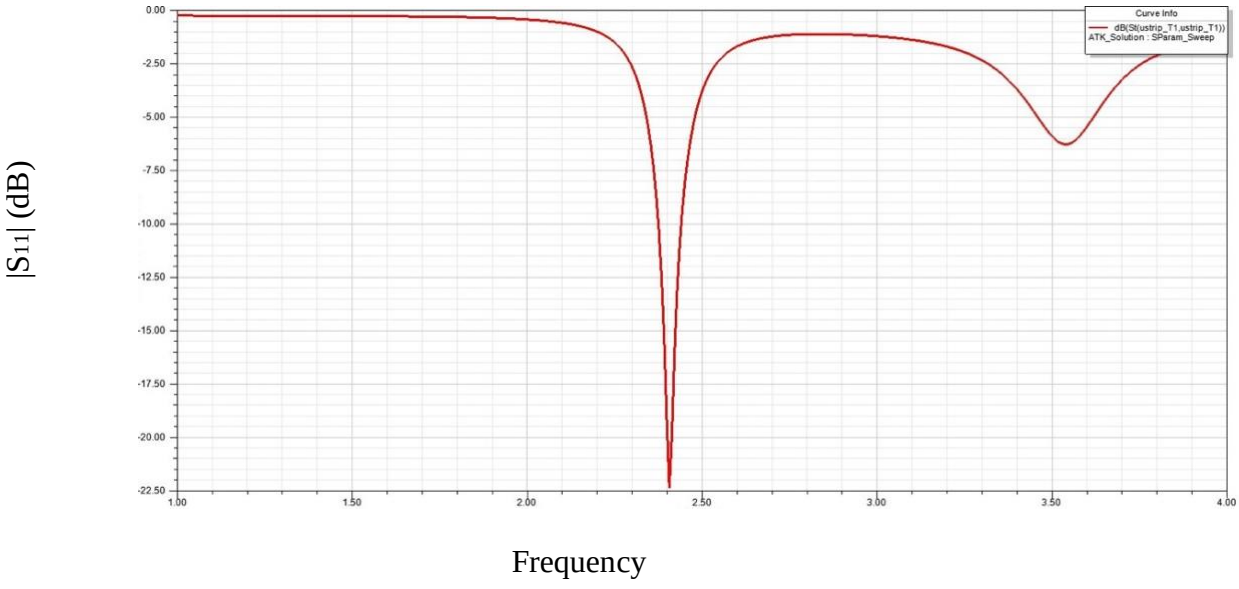

the electrical properties of vacuum and fat are completely different. The dimensions of the model shown in Figure 1 are shown in Table II. The return loss curve of the optimized antenna can be seen in Figure 3.

Table II. Parametrized dimensions of CBSA in fat

Dimension	Initial value	Final value
Slot length	5.2 cm	3.6 cm
Slot width	0.21 cm	0.06 cm
Feed Offset	1.8 cm	0.1 cm
Stripline width	0.15 cm	0.22 cm
Stripline offset length	0.53 cm	1.1 cm
Cavity length	8.1 cm	4.8 cm
Cavity width	3.2 cm	2.5 cm

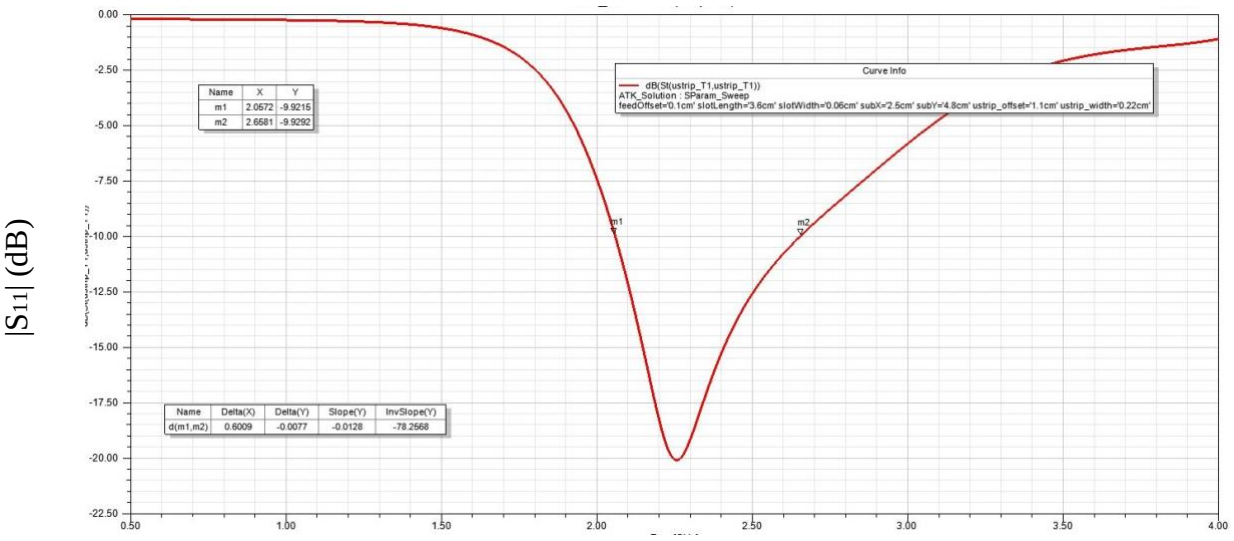

2.1.c Thermal Analysis

The model is already set up in HFSS to prepare it for thermal analysis. The HFSS geometry and the associated solution data should be transferred to ANSYS Workbench and the thermal analysis carried out in ANSYS Workbench. The thermal properties of the materials should be

introduced to the software. [10] Thereafter, heat dissipation should be specified by assigning convection to the exterior surfaces of the structure. In addition, it should be introduced into software which objects introduce heat effect to calculate the thermal properties. There are two types of imported loads: heat flux, heat generation. The designed model should have both, because there exist volume losses caused by currents flowing in the volumes of lossy dielectrics and surface losses caused by currents flowing in the volumes of lossy dielectrics. After completing these steps, the temperature of the entire model can be displayed. However, the thermal demonstration of CBSA was not satisfactory. The temperature increases from 37 °C to 37.13 °C.

In the antennas for telecommunications and broadcasting, input impedance, radiation pattern and radiation efficiency are among the important factors for performance evaluation. In contrast, in antennas for thermal treatment, it is the specific absorption rate (SAR) and the temperature distribution in the body that are the important criteria.[11]

Figure 4: Simulated SAR distribution of CBSA

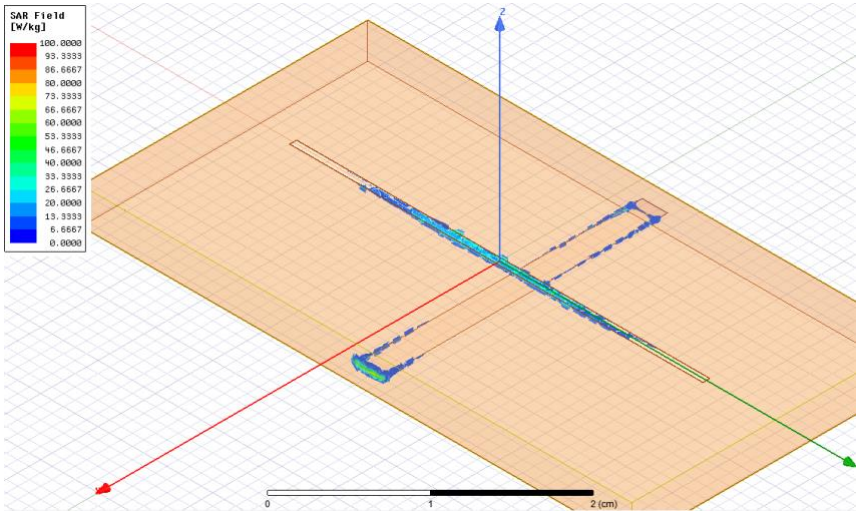

Figure 4 shows the simulated SAR distribution around the CBSA. Here the CBSA is inserted into human fat tissue ($\varepsilon_r = 5.28$, $\sigma = 0.102$ S/m at 2.4 GHz) [12]. The relative high SAR region exists only around the slot and the tip of the microstrip. But the region is so small that a prototyped antenna is going to definitely fail the heating of the surrounding tissue.

Having understood the fact that a CBSA cannot provide a good heating, a literature review has done to understand which type of antennas have been developed and reported in the literature. After literature review, it is decided to model the coaxial-slot antenna. [13]

2.2 Modelling of Coaxial-Slot Antenna

The coaxial-slot antenna is composed of a thin semi-rigid coaxial cable. Some ring slots are cut on the outer conductor of the thin coaxial cable and the tip of the cable is short circuited. The operating frequency is 2.45 GHz, which is one of the Industrial, Scientific, and Medical (ISM) frequencies. Figure 5 and Table 3 show the basic structure and the structural parameters of the antenna. The performance of modelled antenna is judged by its thermal analysis and SAR distribution.

Figure 5: Basic structure of the coaxial-slot antenna [14]

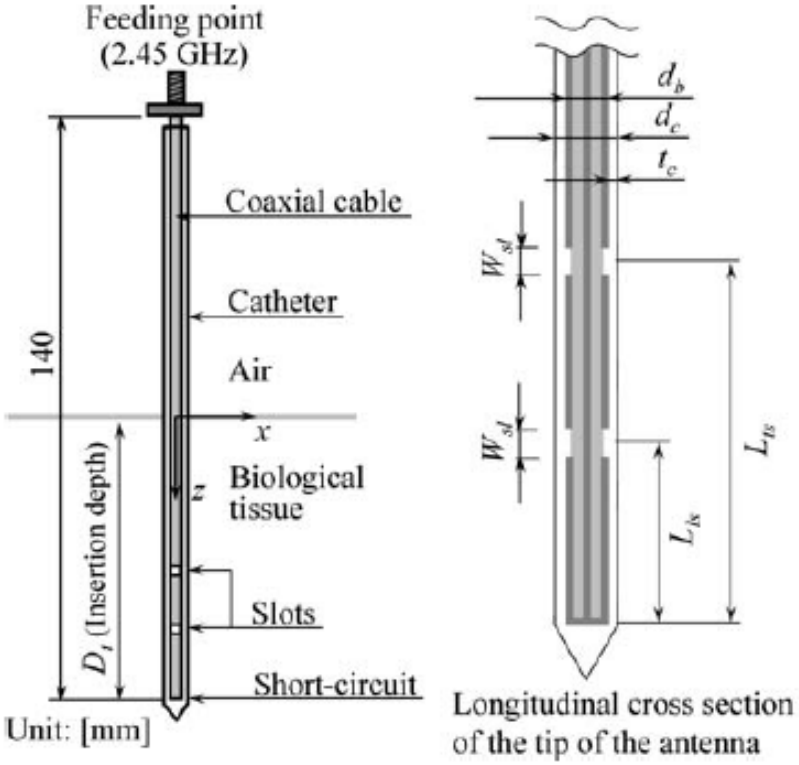

Table III. Structural parameters of the coaxial-slot antenna with two slots [15]

d_b (diameter of the antenna) [mm]	1.19
d_c (external diameter of the catheter) [mm]	1.79
t_c (thickness of the catheter) [mm]	0.3
L_{ts} (length from the tip to the center of the slot close to the feeding point) [mm]	20.0
L_{ls} (length from the tip to the center of the slot close to the tip) [mm]	10.0
W_{sl} (width of the slot) [mm]	1.0
ε_{rc} (relative permittivity of the catheter)	2.6

Modelling of this antenna gives the opportunity to check my thermal analysis setup. The coaxial-slot antenna was already modelled and analyzed electrically and mechanically. Comparing my simulated results and given results in the paper. [16] I concluded that my thermal analysis setup mentioned in previous section of this chapter is successful. Figure 6 shows the geometry of modelled antenna in HFSS and figure 7 shows its simulated SAR. The observation planes are x-z and x-y planes. The high SAR region exists only around the tip of the antenna. One can compare the simulated and measured SAR region in figure 8, they are similar as expected.

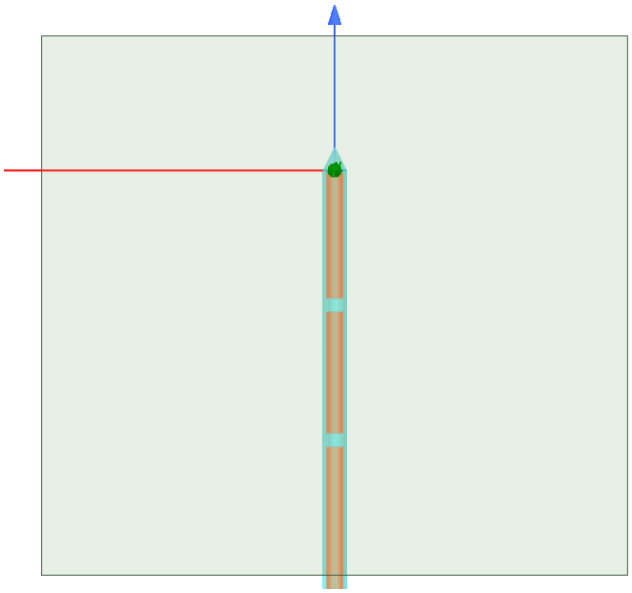

Figure 6: Modelled coaxial-slot antenna

b) xz plane

a) xy plane

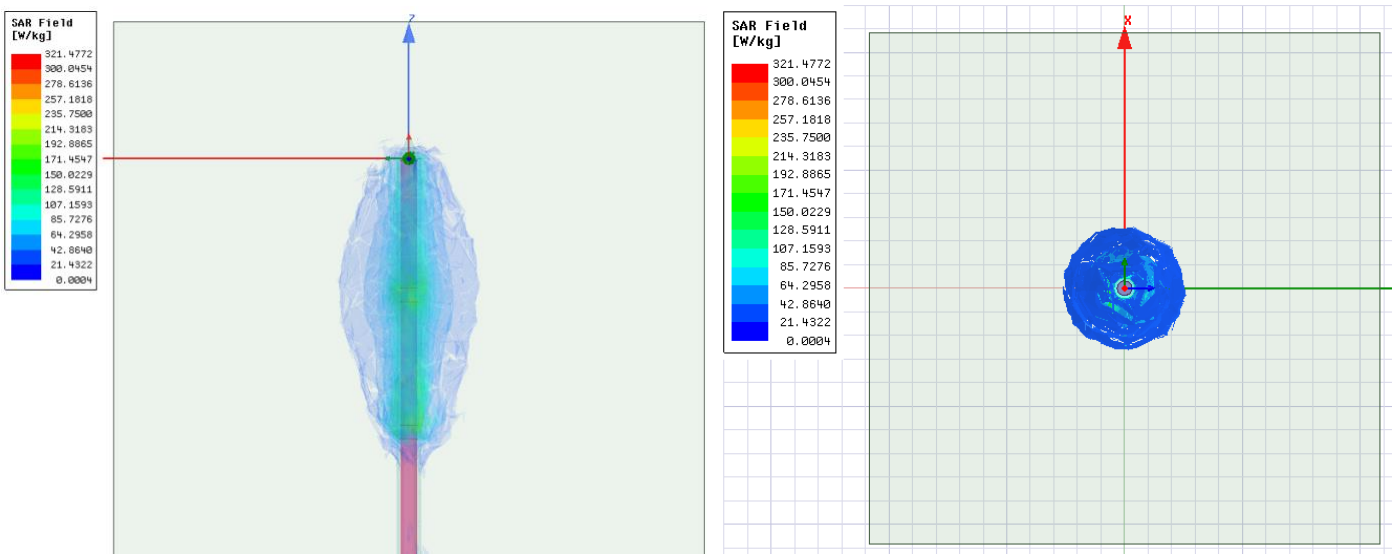

Figure 7: Simulated SAR distribution of the modelled antenna

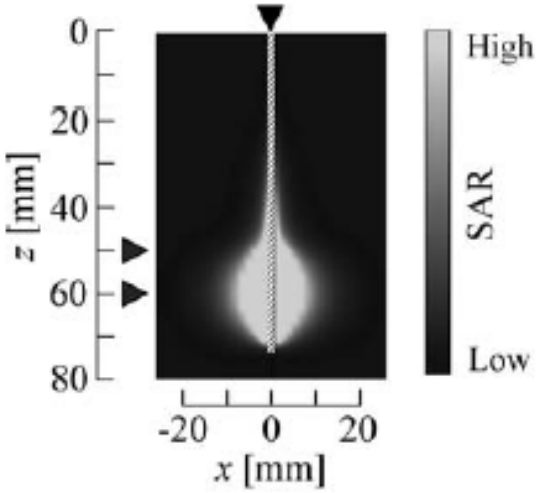

Figure 8: Measured SAR distribution [17]

After observing the SAR values of modelled antenna are satisfactory, the thermal analysis of the modelled antenna should be done. The HFSS geometry and the associated solution data is transferred to ANSYS workbench and the thermal analysis carried out in ANSYS Workbench. For the simulations the net input power of the antenna is 5.0 W. The heating time is 600s. In addition, the initial temperature of the biological tissue (muscle) is 37 ºC. The surrounding tissue's electrical and thermal properties are : ε_r (relative permittivity)= 47 , σ (conductivity in S/m), = 2.21, c (specific heat in J/ Kg.K) = 3500, κ(thermal conductivity in W/m.K) = 0.60, ρ(density in kg/m3) = 1020. [18] The figure 9 shows the simulated temperature distribution and the figure 10 shows the measured temperature distribution. They are also similar as expected.

Figure 9: Simulated temperature distribution

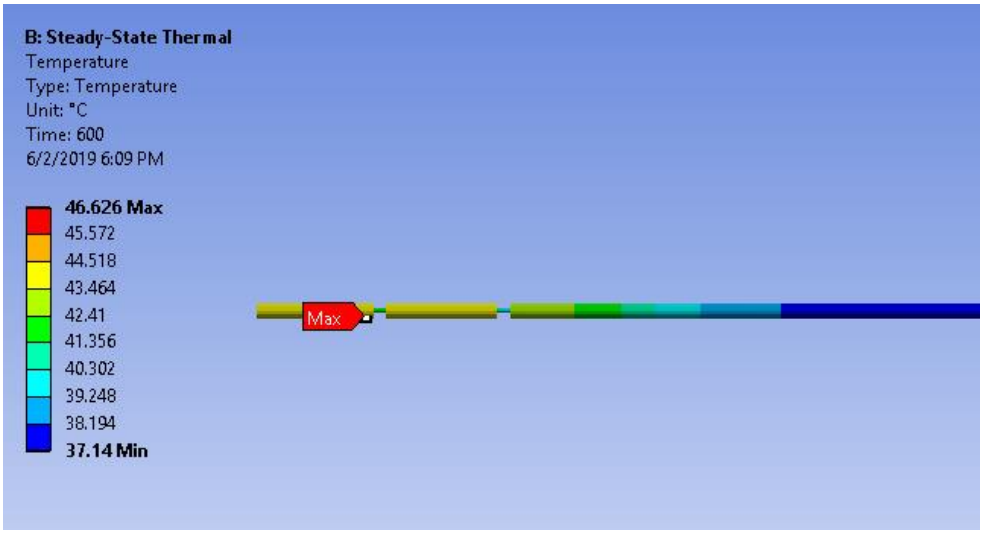

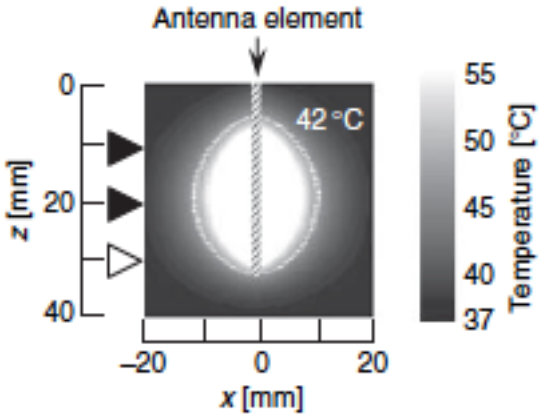

Figure 10: Measured temperature distribution

After observing that my simulation works with no problem, I started to think about the question what type of antenna I can use in my project for a better heating simulation in other terms for an antenna with large SAR values. After meetings with my principal investigator and some literature review, I decided to use C type slotted antenna.

2.3 Design of an antenna with C type slots

The designs of C type slotted antenna and coaxial-slot antenna are similar. This is why one should expect large SAR values in the neighborhood of the antenna. In figure 11 one can see the basic structure of the designed antenna. The substrate used in this antenna design is Rogers RO3210 which has the electrical property $\varepsilon_r = 10.2$. The surrounding tissue is cortical

bone (ε_r = 1.14, σ =0.385 S/m). [19] The parameters of the designed antenna can be seen on the table IV.

This antenna is simulated inside the hip implant designed by Sema Dumanlı Oktar. On figure 12 one can see the combination of the hip implant and designed antenna. On figure 13 one can see the simulated SAR distribution of the designed antenna. The observation planes are xy and xz planes. The high SAR region exists around the slots of the antenna and the regions are far wider than the SAR regions of my first antenna (cavity backed slot antenna).

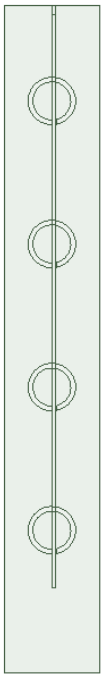

Figure 11: Basic structure of the designed antenna

Table IV. Parameters of the antenna with C type slots

Size of antenna	10 mm x 70 mm
Thickness of substrate	1.28 mm
Feed length	60 mm
Inner radius of C type slot	2 mm
Outer radius of C type slot	2.5 mm

Figure 12: Combination of the hip implant and designed antenna

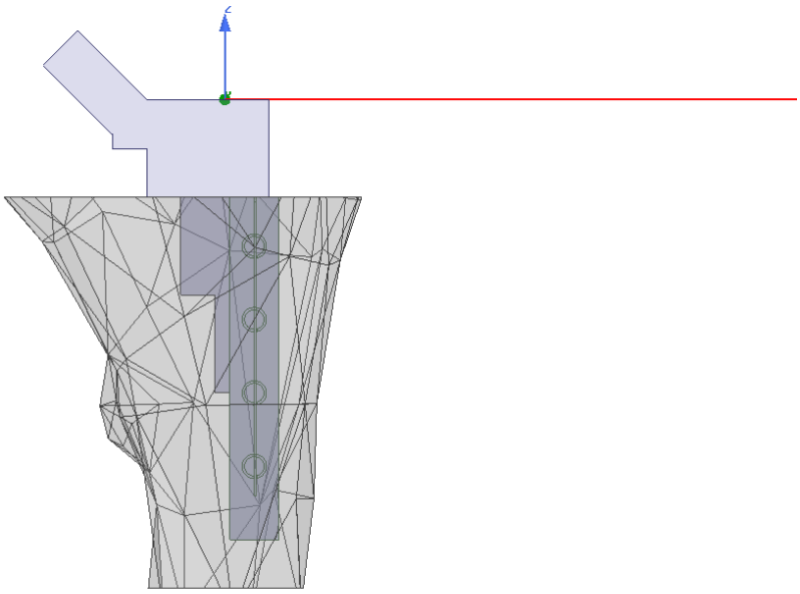

Figure 13: Simulated SAR distribution of the designed antenna

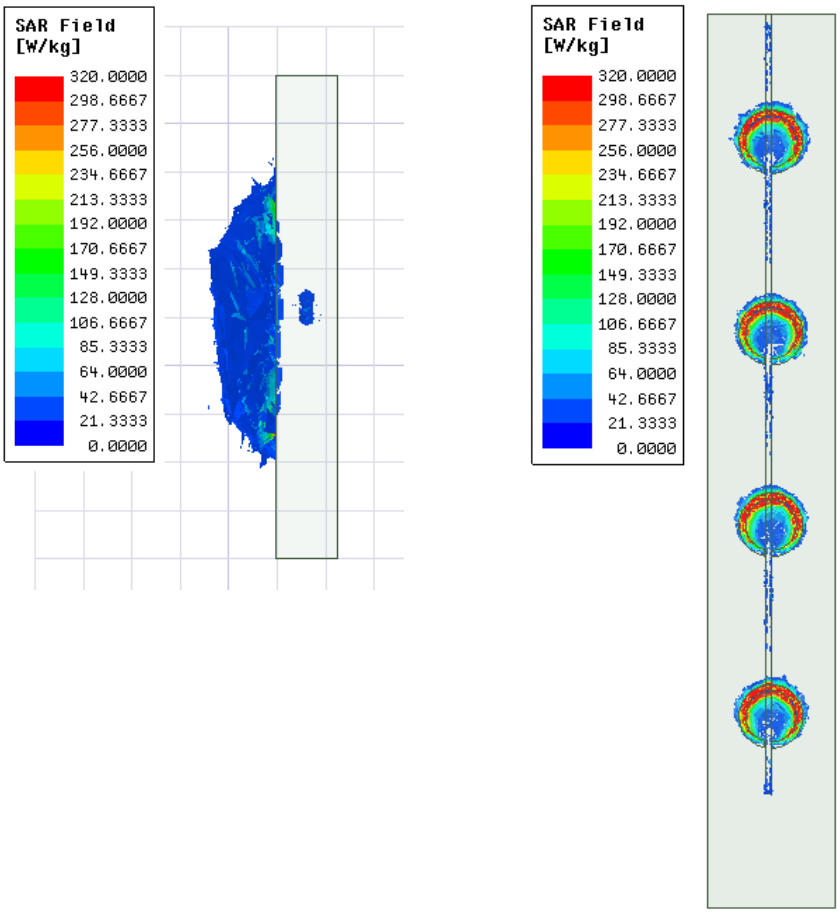

The HFSS geometry and the associated solution data is transferred to ANSYS Workbench and the thermal analysis carried out in ANSYS Workbench. The thermal properties of the materials are also introduced to the software. After completing necessary steps mentioned before, the temperature of the entire model can be displayed. The temperature around the slots increases from 37 °C to 38.53 °C. Even though the result is much better than the result of my first designed antenna, it does not meet the aforementioned evaluation criterion for the microwave hyperthermia, whether the 1 mm neighborhood of the designed antenna can be heated up to 40 °C.

CHAPTER 3

METHODOLOGY AND ANALYSIS (EE 492)

In the first part of the project (EE 491), great progress had been made. You can review my previous reports to see what I did. At the beginning of the semester a meeting was held with my supervisor and we talked about what we are going to do this semester.

It was important to test that we did the thermal analysis correctly. The coaxial-slot antenna of Koichi Ito is designed and tested accordingly. The further explanation can be found on the final report of first part of the project.

The first task of this semester was to design a prototype antenna to test heating at different frequencies. One can see the prototype antenna and measurement setup on Figure 14. It is a circular slot antenna. To operate this antenna at the different frequencies (0.5 GHz to 2.5 GHz) one should definitely change the size of the slot in other words change the diameter of the inner circle and the width of the slot. One can also the change of the slots of antennas operating at 2 GHz and 2.5GHz on Figure 15 and Table V.

This first task was very critical, because doing this we can find the optimum operating frequency value of the antenna which results in perfect SAR distribution. This process is also called heating optimization. It is clear that the heating occurs because of near field losses and it is frequency dependent. We have the possibility to test different frequencies unlike the Koichi's circular slot antenna, because for our purposes only the specific small neighborhood of the antenna is important, not the depth or area of the heated region.

To determine the antenna's working frequency is also important because I should also get a transmitter which works at this frequency value. So, it is an initial step for prototyping.

This was a simple setup as one can also see on Figure 14, but things did not go the way we wanted. We concluded that testing different frequencies is difficult in this setup. The limitation was that I could not change the antenna size as much as I wanted. To overcome this obstacle, it was decided to use a miniaturized antenna. The setup can be seen on Figure 16. This

design is initially made by my supervisor Prof. Sema Dumanlı Oktar. It is a complex design and was a little bit hard to understand. But after spending some time on the model I got it.

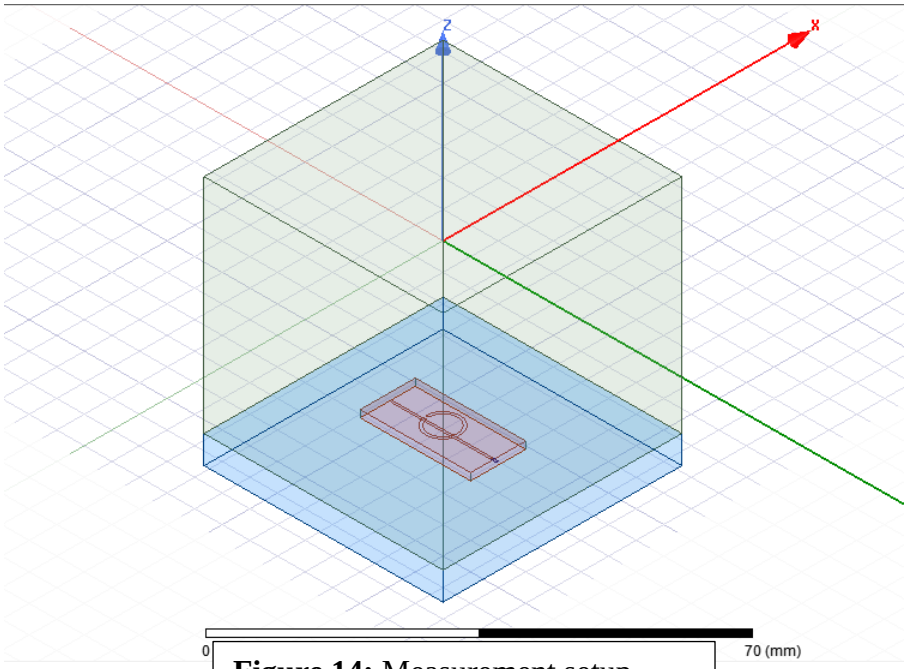

Figure 14: Measurement setup

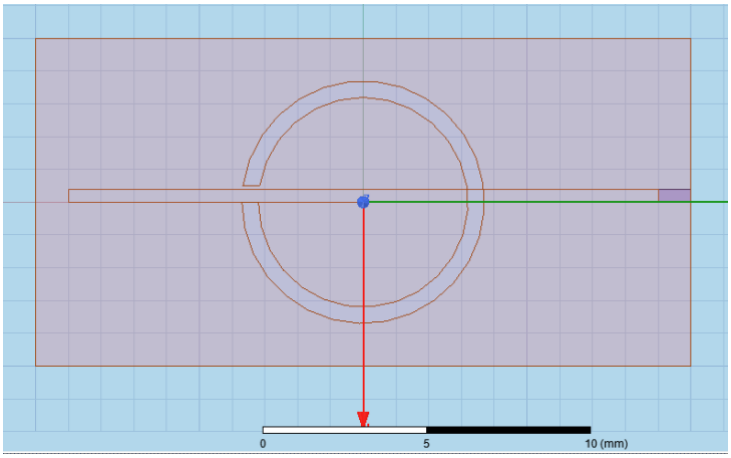

Figure 15.a : Operating at 2.0 GHz

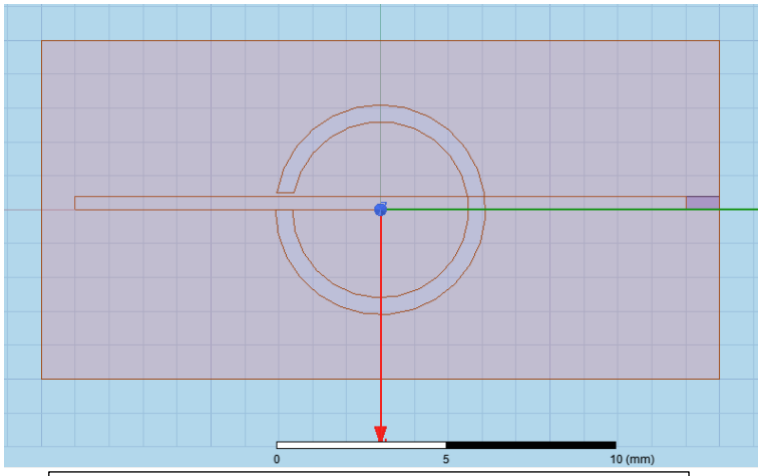

Figure 15.b : Operating at 2.5 GHz

Operating Frequency	feedLength	Innerslot length	Slotwidth
1.5 GHz	63 mm	4.3 mm	0.5 mm
2.0 GHz	63 mm	3.2 mm	0.5 mm
2.5 GHz	63 mm	2.6 mm	0.5 mm

Table V: Parameters used on the model

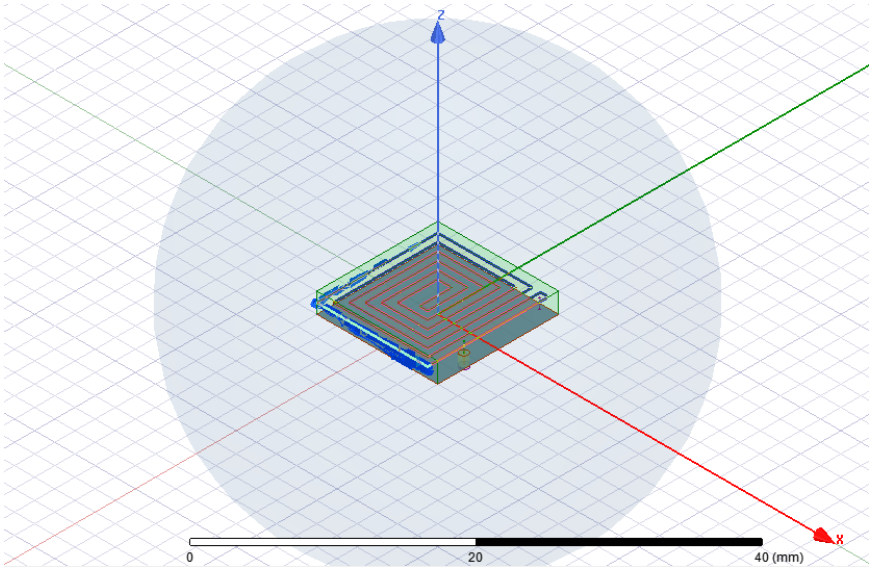

Figure 16: Measurement setup

The antenna is inside a spherical medium which is human bone cortical. The antenna consists of a labyrinth like slot, a ground plane, implant substrate and feeding mechanism. An optimization process has done like before. Only by changing the slot width of the labyrinth like slot the antenna is matched at different frequencies. You can see the related S-parameters plot below.

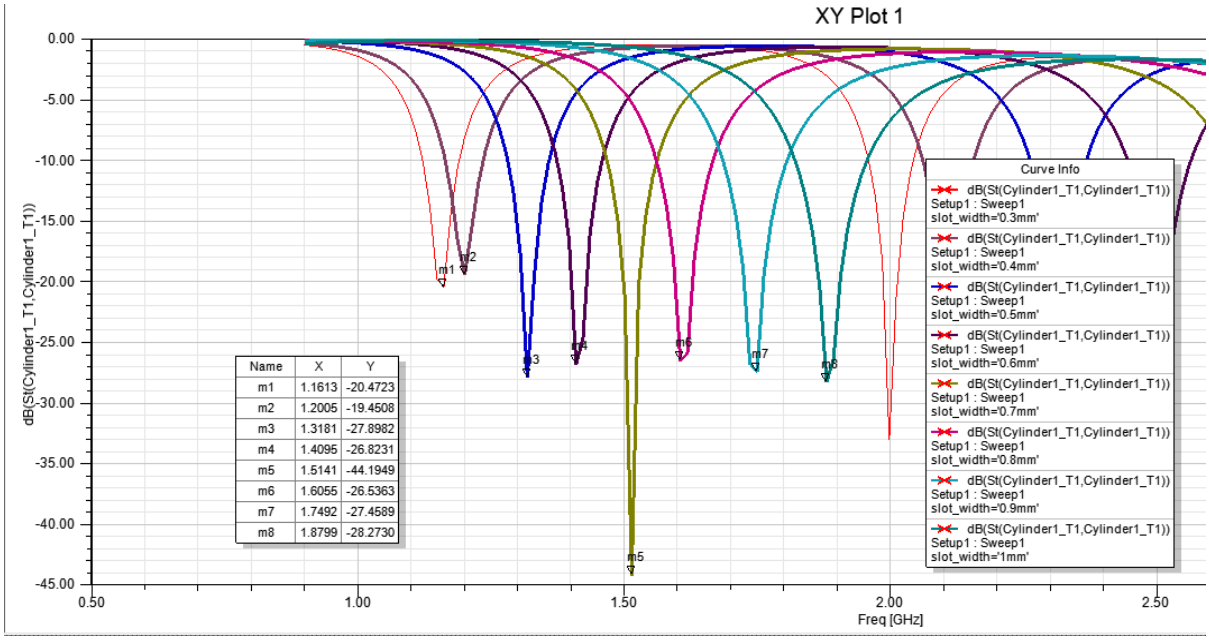

Figure 17: S parameters plot

One can see here the antenna has perfectly matched to operate at different frequencies. After deciding the slot widths of the labyrinth like antennas and their corresponding frequencies (see Table **VI**). Specific simulations at specific frequencies were performed and electric fields were calculated accordingly. The SAR plots were drawn and interpreted with my advisor. You can see the SAR plots seen from different angles below. (**Figure 18 to Figure 25**)

Working frequency	**Slot width**
1.16 GHz	0.3 mm
1.20 GHz	0.4 mm
1.31 GHz	0.5 mm
1.41 GHz	0.6 mm
1.51 GHz	0.7 mm
1.60 GHz	0.8 mm
1.75 GHz	0.9 mm
1.88 GHz	1.0 mm

Table VI: Slot widths and corresponding working frequencies

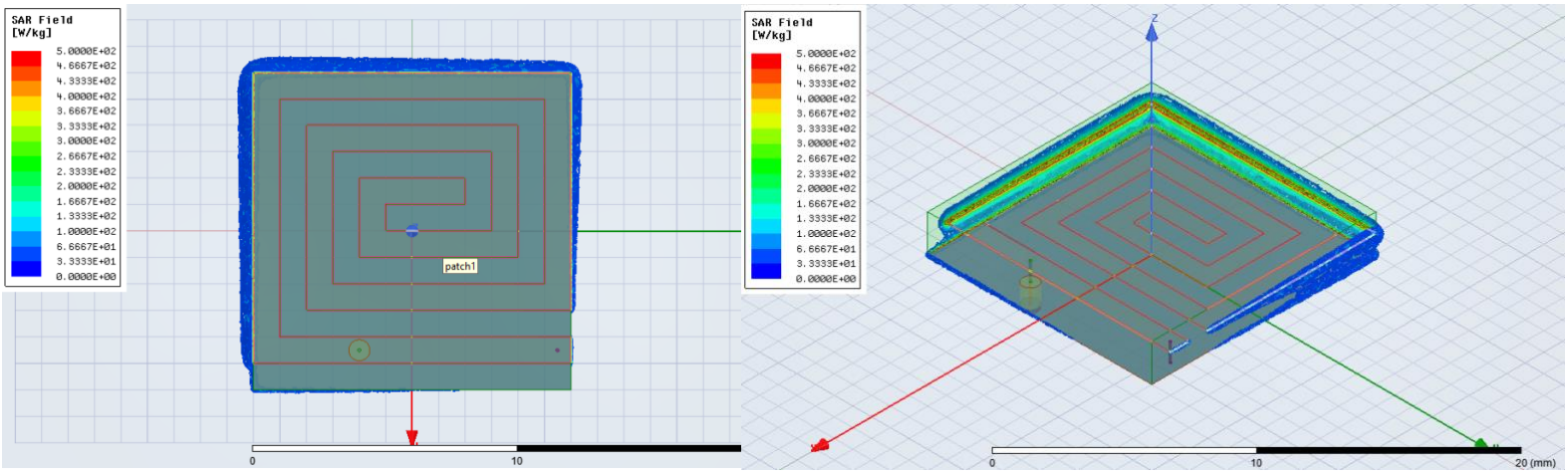

Figure 18: SAR distributions at 1.88 GHz seen from different angles

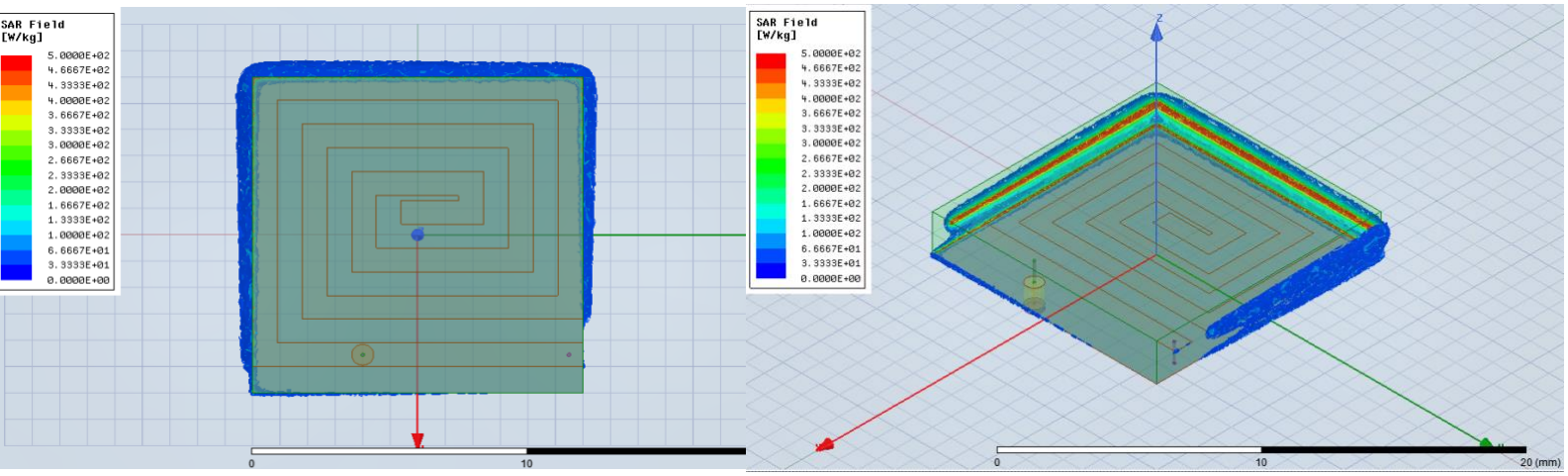

Figure 19: SAR distributions at 1.75 GHz seen from different angles

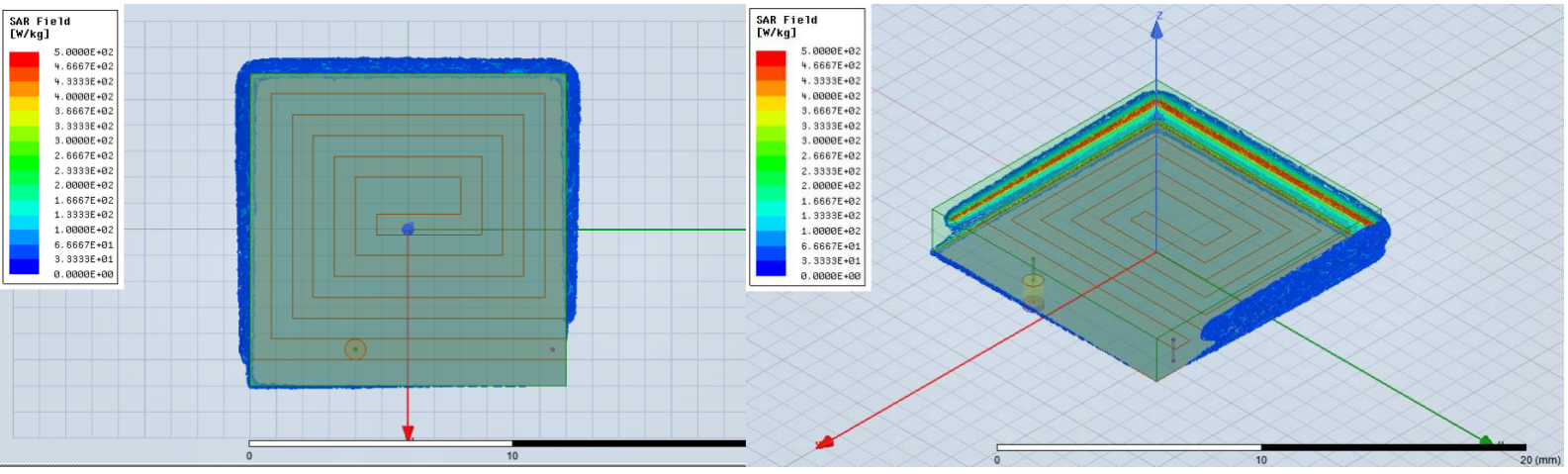

Figure 20: SAR distributions at 1.60 GHz seen from different angles

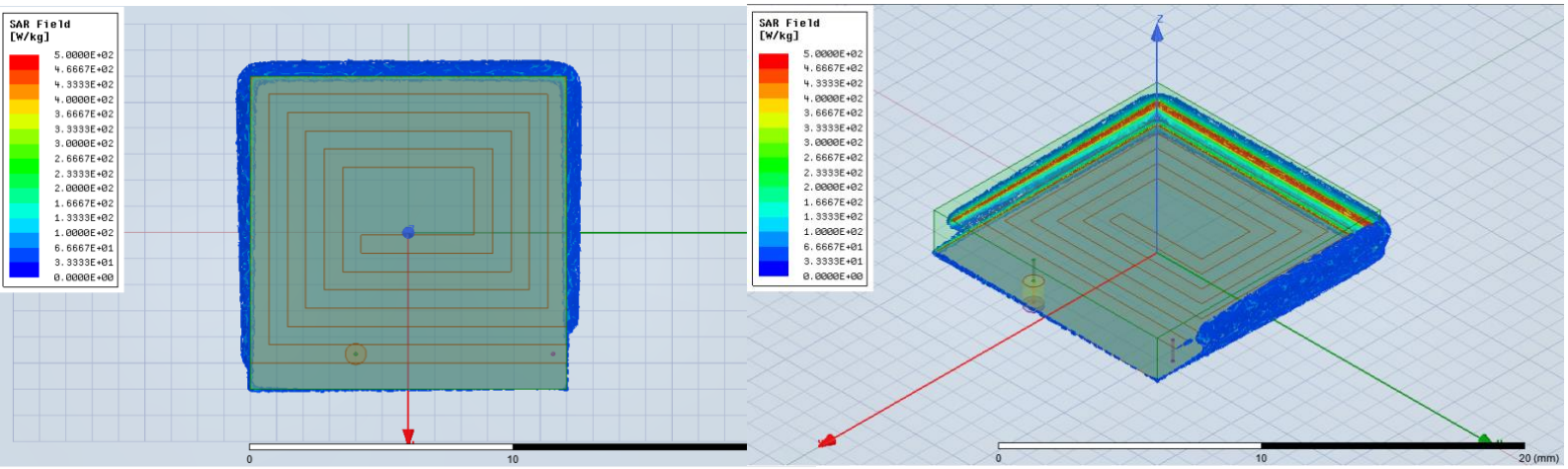

Figure 21: SAR distributions at 1.51 GHz seen from different angles

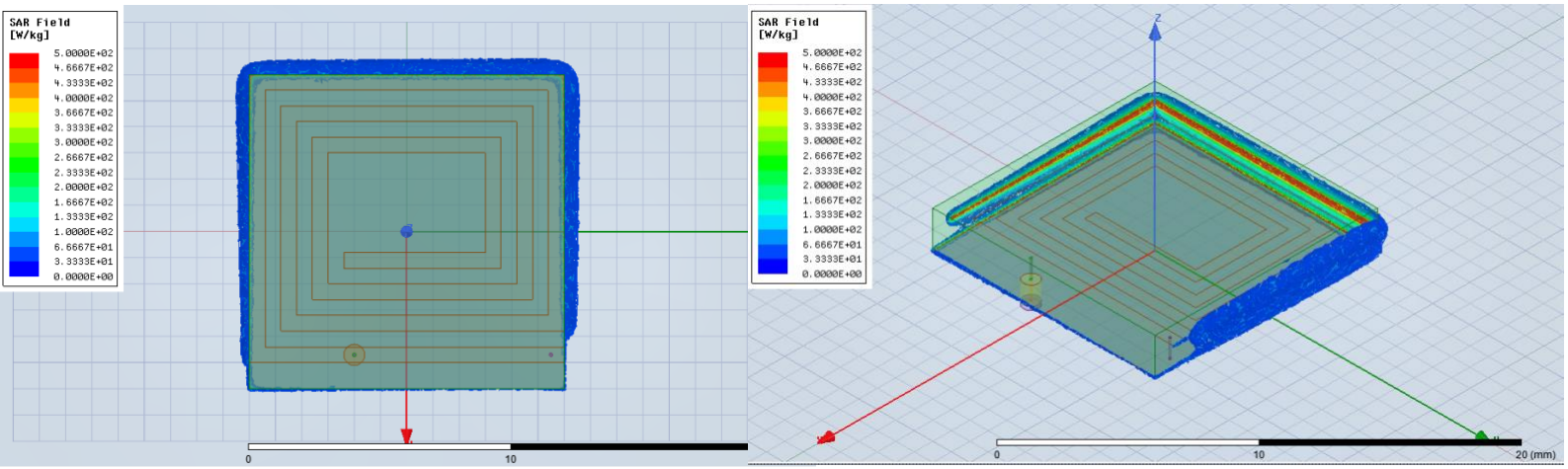

Figure 22: SAR distributions at 1.41 GHz seen from different angles

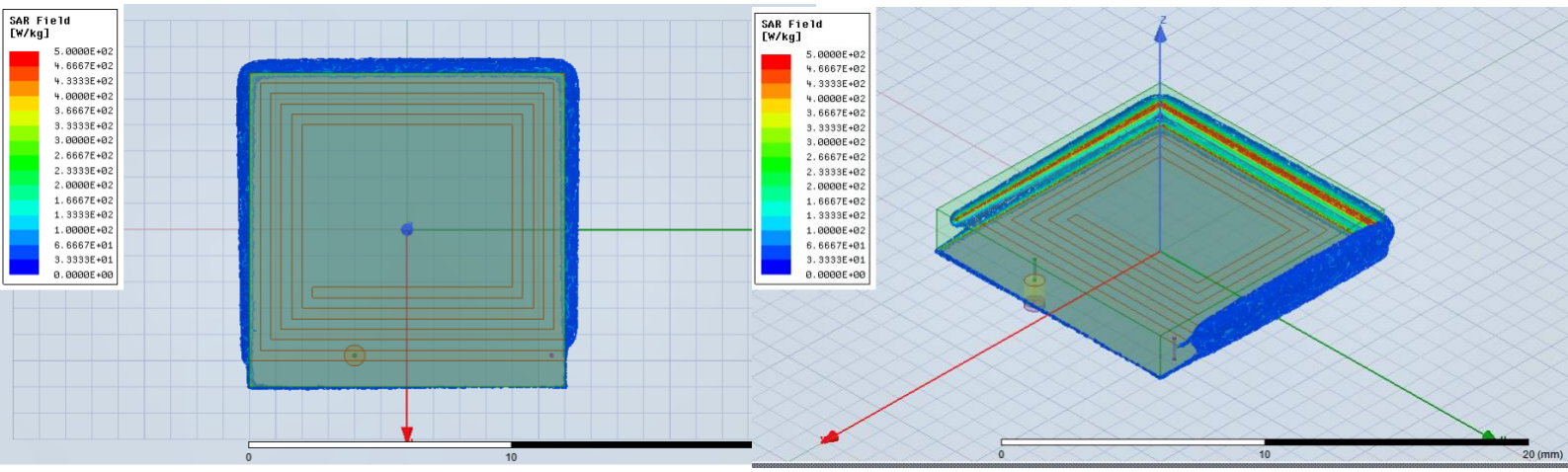

Figure 23: SAR distributions at 1.31 GHz seen from different angles

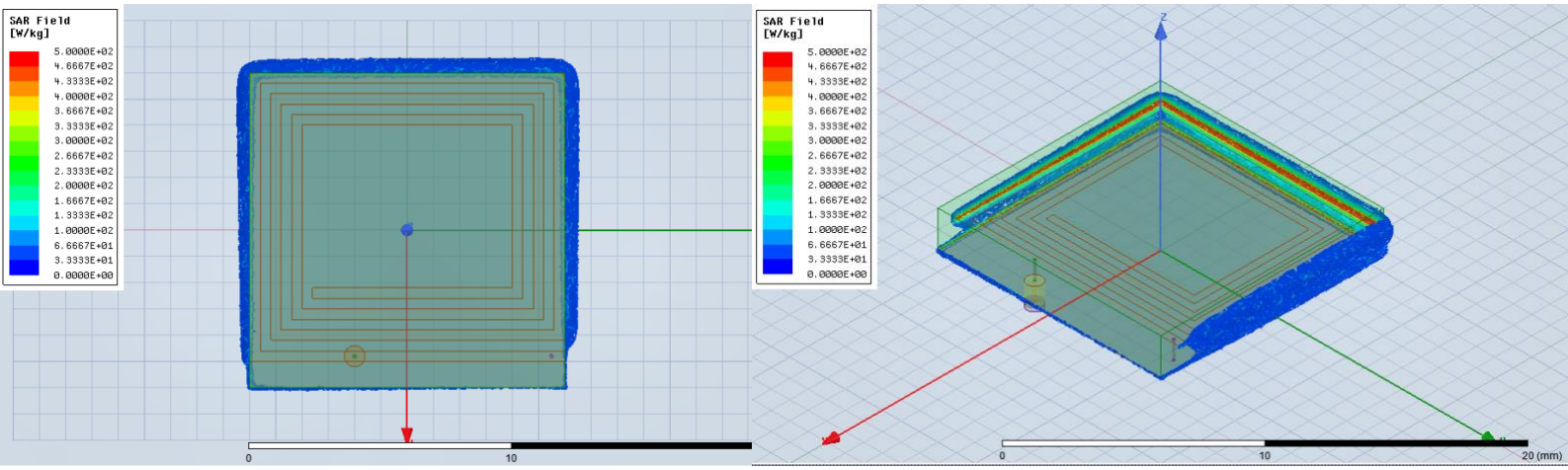

Figure 24: SAR distributions at 1.20 GHz seen from different angles

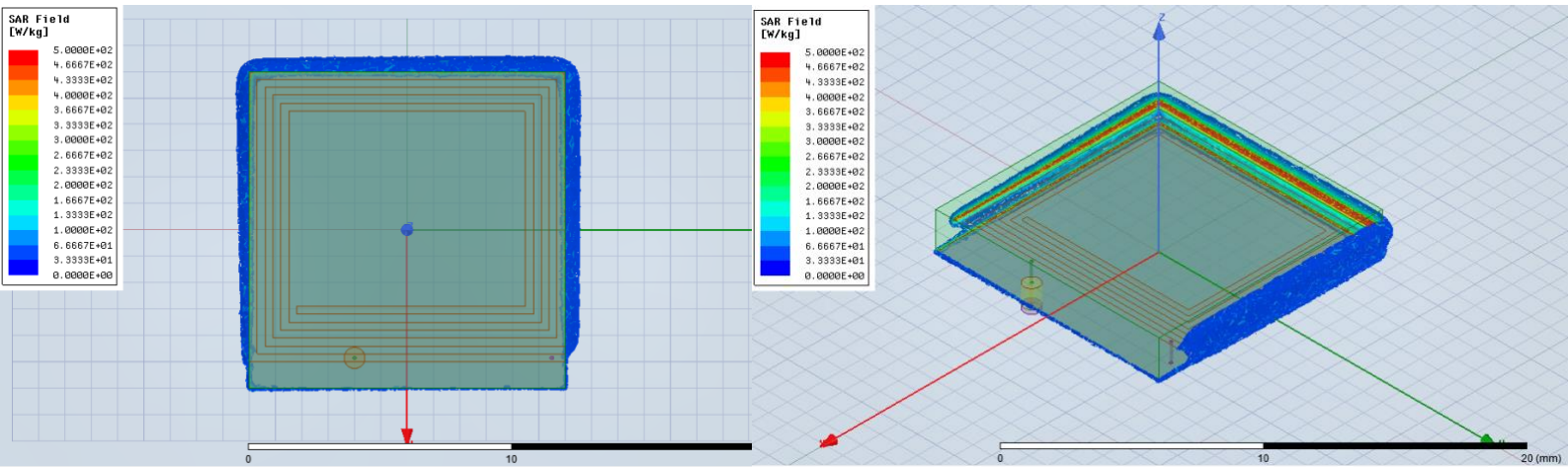

Figure 25: SAR distributions at 1.16 GHz seen from different angles

According to these results, one can obtain a better SAR distribution at lower frequencies.

CHAPTER 4

MEASUREMENT SETUP

At this stage, I thought about how to take measurements after producing the antenna. In the previous stage, the antenna I had prototyped and optimized was in the human bone cortical tissue, but we do not want to produce an antenna that will work in the human bone cortical tissue and observe if it will heat it around. Bacteria grow in a medium called serum between the implant and bone. The dielectric properties of this gely structure are quite different from human bone cortical. So, we decided to change the material to be used from human bone cortical to human fat, so that the dielectric and thermal properties are close to the serum and phantom production is easy.

I changed the design in the simulation program to fit it in the measurement cup. The feeding structure is also added. Antenna optimization was done again. The following pictures show the features of the designed antenna.

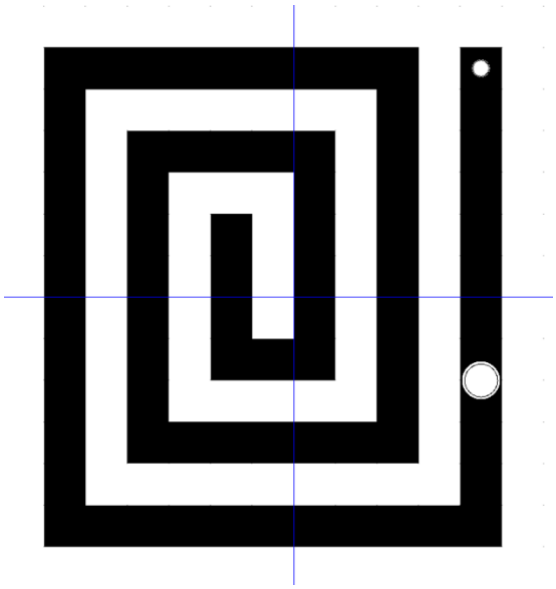

Figure 26: Antenna top view

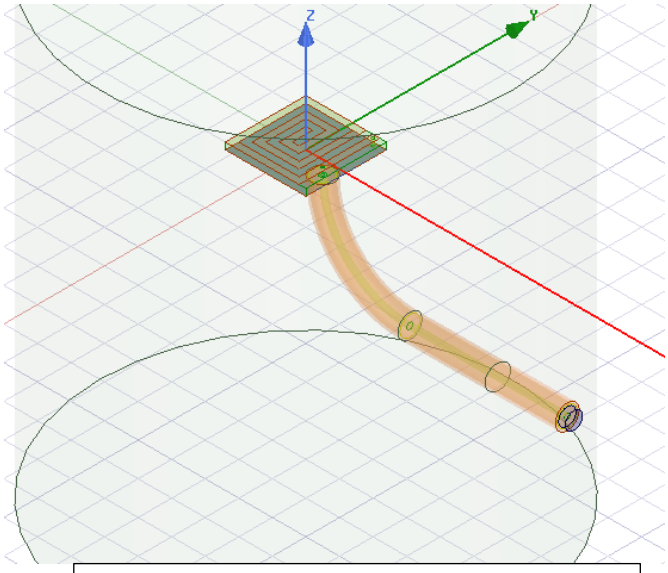

Figure 27: Designed antenna on HFSS

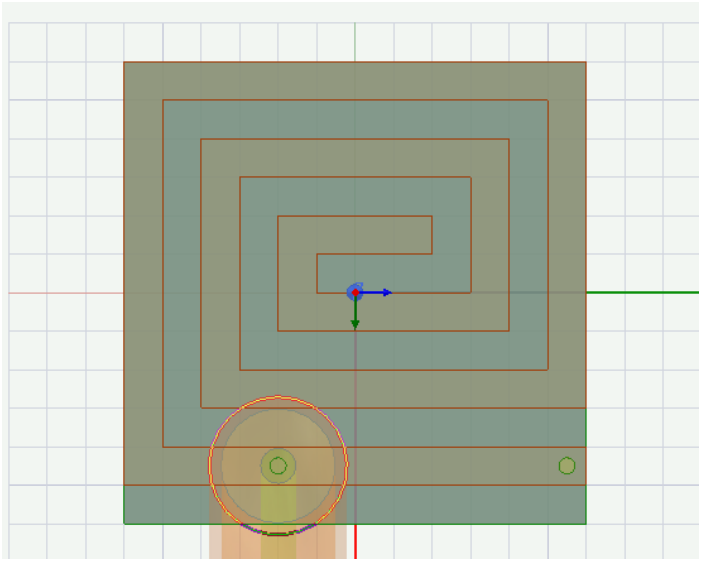

Figure 28: Designed antenna on HFSS (top view)

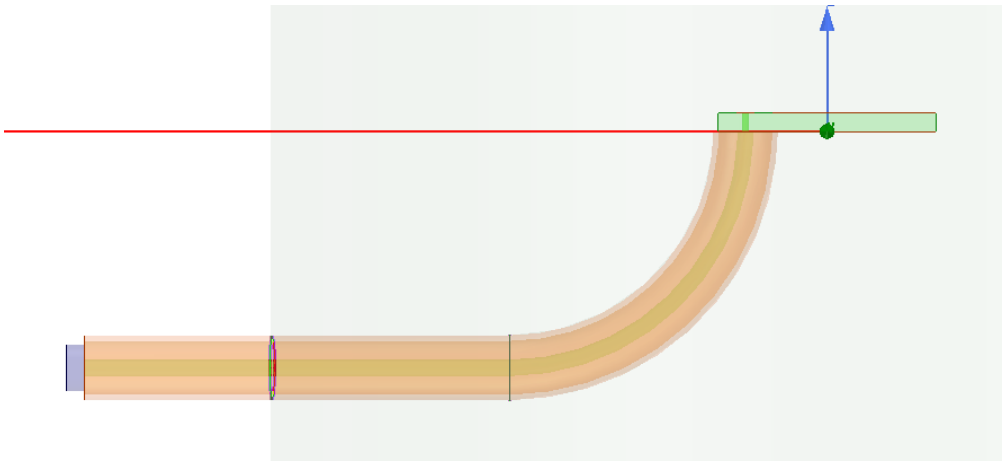

Figure 29: Designed antenna on HFSS (side view)

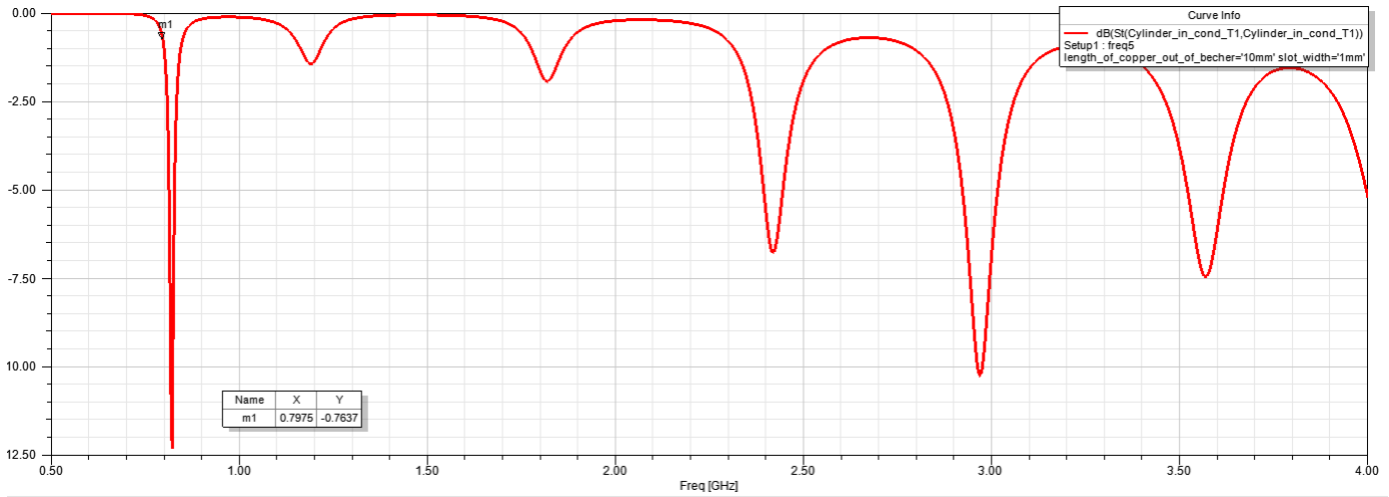

Figure 30: Simulated S_{11} vs frequency

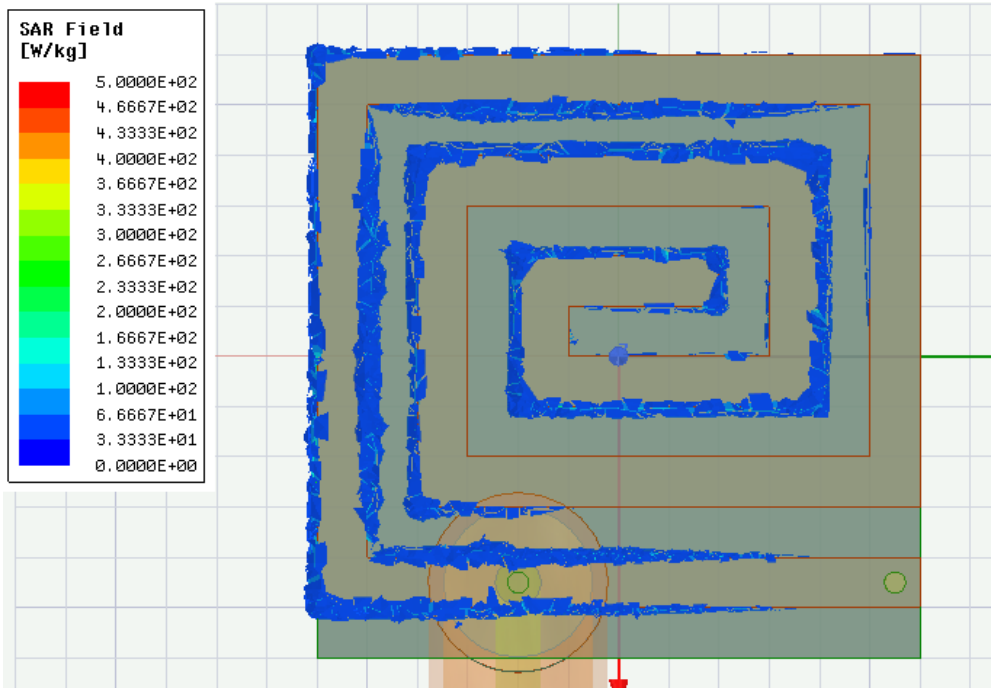

Figure 31: Simulated SAR distribution of the designed antenna

The resonance frequencies of the antenna designed according to the S parameter analysis are shown in the Figure 30. According to previous experiments, the SAR values at the lowest frequency were higher, so I decided to feed the antenna at the lowest frequency resonance which is 0.83 GHz. The Figure 31 shows the simulated SAR distribution. SAR calculations are based

on the assumption that the antenna is supplied with a power of 6 dbm. This is the maximum amount of power the VNA in the BOUNTENNA lab can provide in signal generator mode.

CHAPTER 5
PHANTOM DEVELOPMENT

The phantom development is based on the article. [11] In this article an artificial breast phantom that has realistic dielectric and thermal properties is presented. My aim was to develop a human fat mimicking material. The developed tissue mimicking materials are designed to not only simulate the dielectric properties, but also the thermal properties of breast tissues.

The process of creating the required tissue mimicking materials includes the three main steps. First, based on the dielectric properties of water, oil, salt, and gelatin, mixtures of different ratios of those materials are used to achieve the required tissues' dielectric properties. Second, the mixtures' dielectric and thermal properties are measured. Third, the mixture ratios, especially for the gelatin, are tuned to control the thermal properties and thus meet both of the tissue's dielectric and thermal properties. But I do not have to follow these steps. In the article, the tissue that mimics the human fat consists of 17 gr gelatin, 40 gr water and 140 gr oil. [11] According to this tariff, an aqueous gelatin solution was produced by mixing gelatin in distilled water, which was then combined with vegetable oil and surfactant that acts as an emulsifier to allow a homogeneous mixture to be made, but because of the ions in the surfactant, it increases conductivity and that is something we do not want. Therefore, more than one experiment should be done and the optimum point should be found.

I did not test the thermal properties of the phantom, but I was able to test the dielectric properties. For this I used the VNA device and a MATLAB code. The MATLAB code calculates the dielectrical properties of the material tested, based on the dielectric properties of deionized water and air. The dielectric properties of the phantom produced in the first step were unsatisfactory. The relative permittivity was higher than expected. The relative permittivity decreases when the oil percentage in the oil-gelatin dispersion increases.

Therefore, 145 grams of vegetable oil was used in the second stage.

The plot showing the dielectric properties of the generated phantom can be seen in the Figure 32. The relative permittivity was in desired range. The conductivity was a little higher than desired value, but I could not think of a way to prevent this, I tried to use as little surfactant as I could.

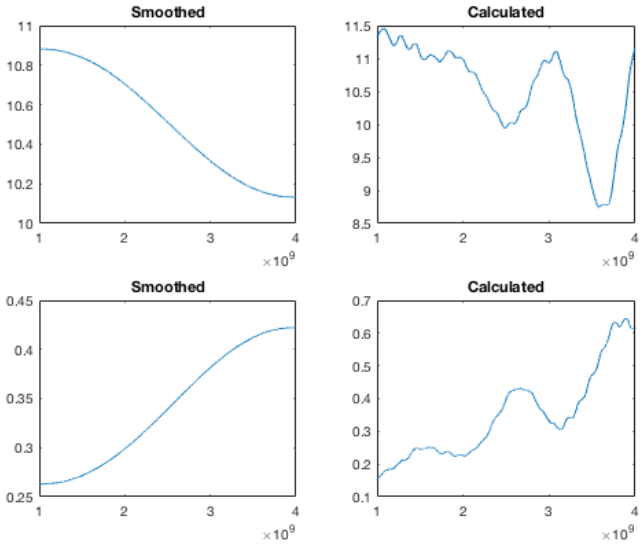

Figure 32.a Permittivity and conductivity values

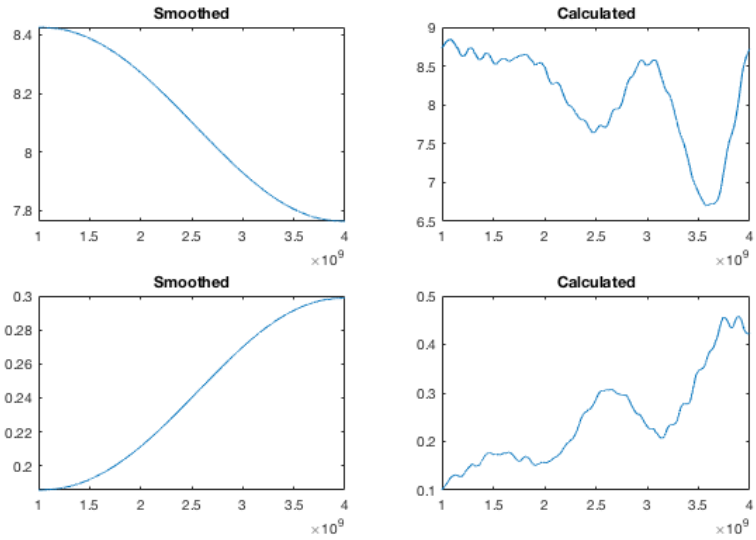

Figure 32.b Permittivity and conductivity values

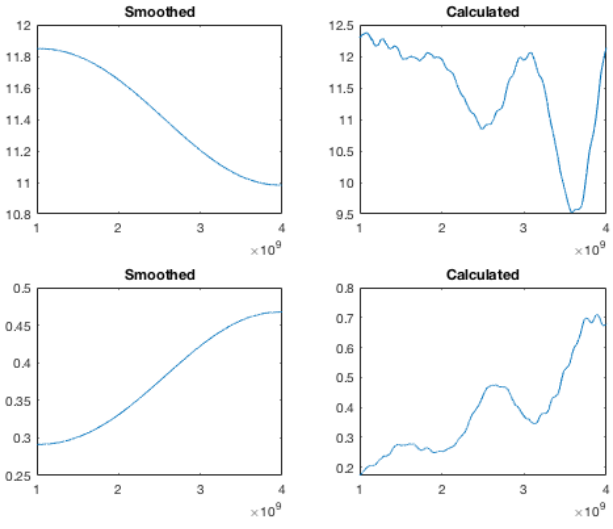

Figure 32.c Permittivity and conductivity values

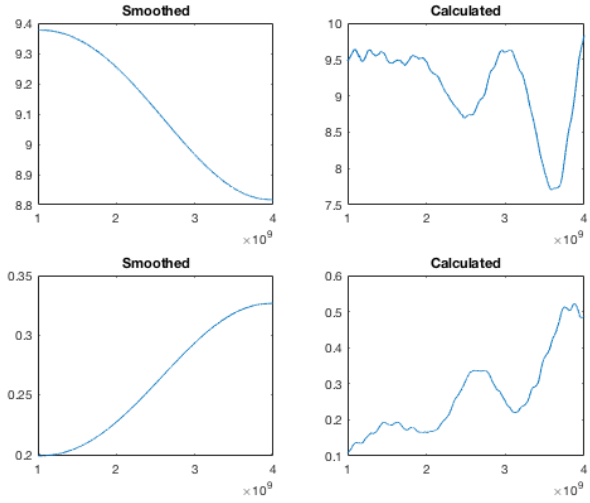

Figure 32.d Permittivity and conductivity values

Figure 33.a Phantom development

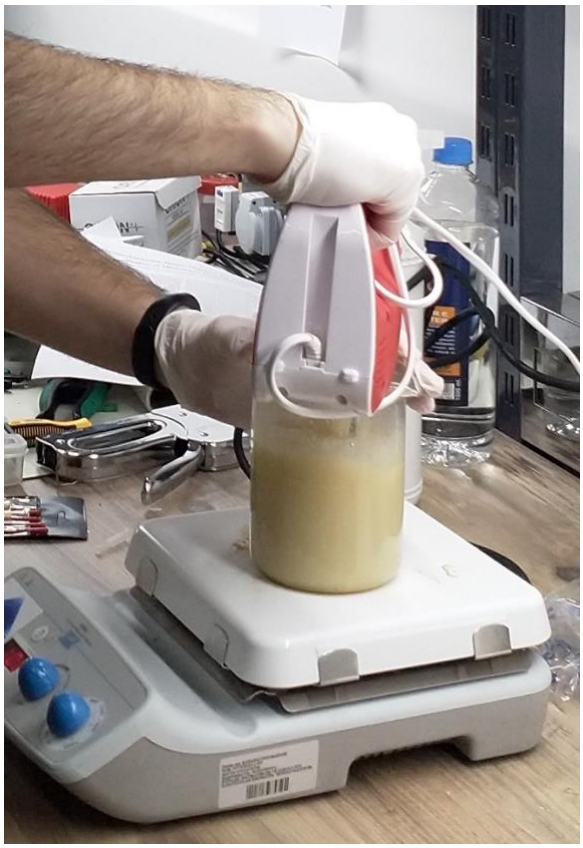

Figure 33.b Phantom development

CHAPTER 6

ANTENNA PRODUCTION

The next task was to produce and install the antenna that would suit the intended measuring system. I learned to use the device called LPKF for this purpose. It is a low-cost introduction to the world of professional in-house printed circuit board prototyping. One can struct single- or double-sided circuit boards, drill holes for through-plating and cut individual boards from the base material with the help of this device. It is an automated device. It can be managed with a pc application. The gerber files of the designed antenna is created and then they are introduced to the LPKF device. In the figure below you can see the photo of the antenna produced.

Figure 34: LPKF device

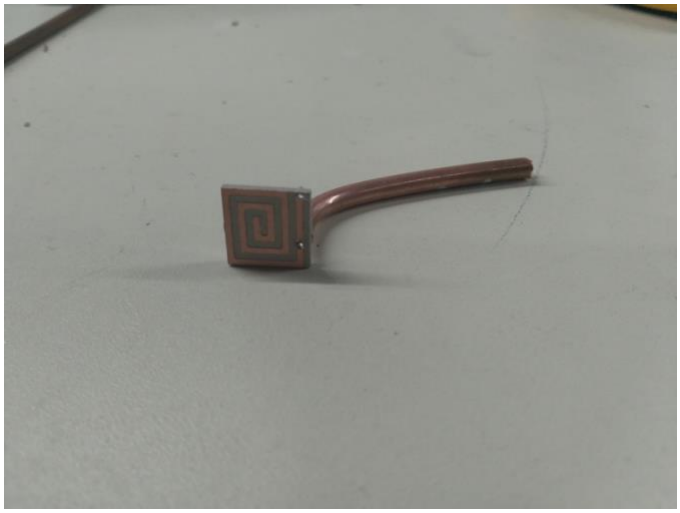

Figure 35: Soldered antenna

After the antenna was produced, the feeding structure was soldered. Then, the antenna was fixed by silicon and looked like in the Figure 36.

Figure 36: Antenna in the measurement setup

The measured S11 parameters of the produced antenna can be seen on Figure …

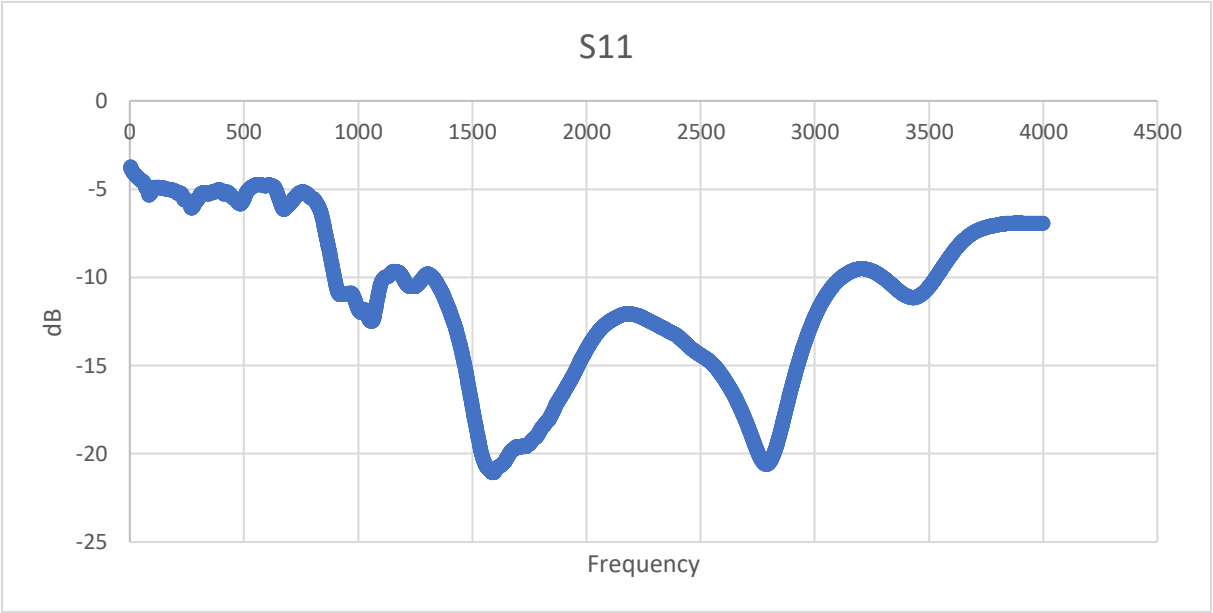

Figure 37: Measured S_{11} parameters vs frequency

CHAPTER 7

THERMAL MEASUREMENT

I told that I am simulating and optimizing my antenna for 6dbm input power. Accordingly, I plot the SAR distribution to 6dBm input power. But I could not observe the heating provided by the input power of 6dbm, because my measuring equipment was inadequate. The thermometer in the laboratory was not sensitive. We tried to measure with a more accurate thermometer, such as a body thermometer, but it did not work. As a last resort we decided to use a thermal camera, but he also had some drawbacks. The area where we want to observe the heat increase is quite small. It is obvious not to observe that such a small area will heat up from the outside. So, we decided to increase the input power. First, we increased it to 50 dbm and then we reduced it to 10 dbm. We used the signal generator from another lab. The results were both thought-provoking and satisfactory, see below.

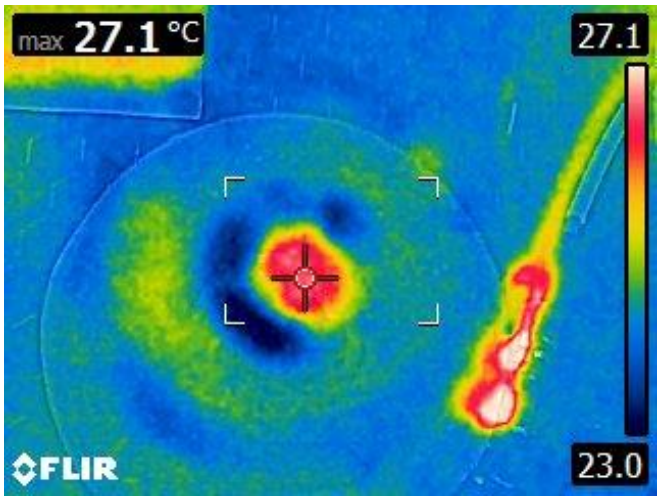

Figure 38.a Thermal camera screenshot input power 50 dBm

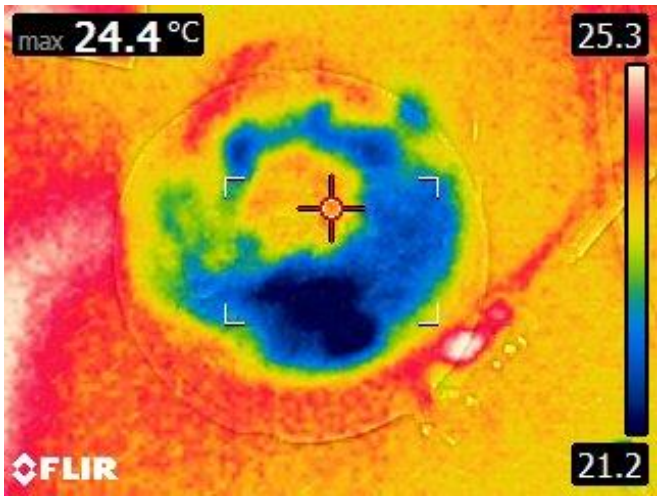

Figure 38.b Thermal camera screenshot input power 50 dBm

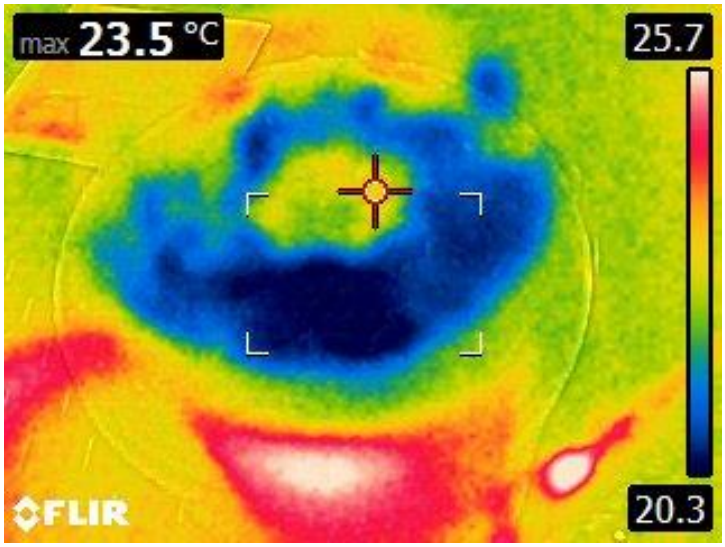

Figure 38.c Thermal camera screenshot input power 10 dBm

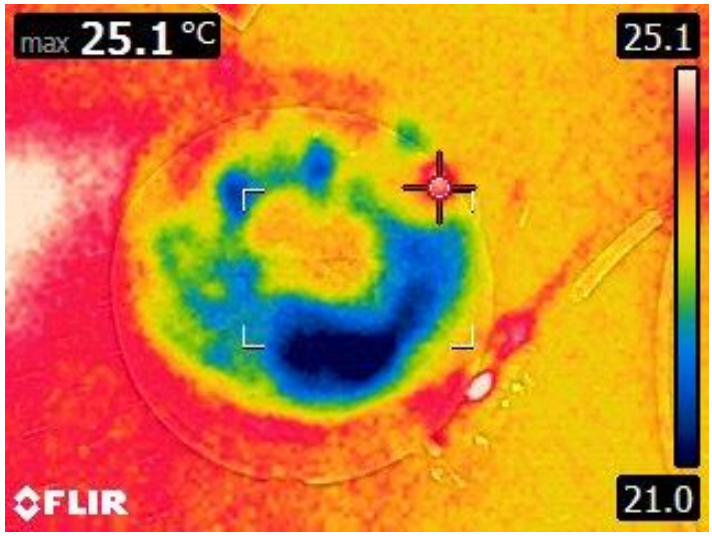

Figure 38.d Thermal camera screenshot input power 10 dBm

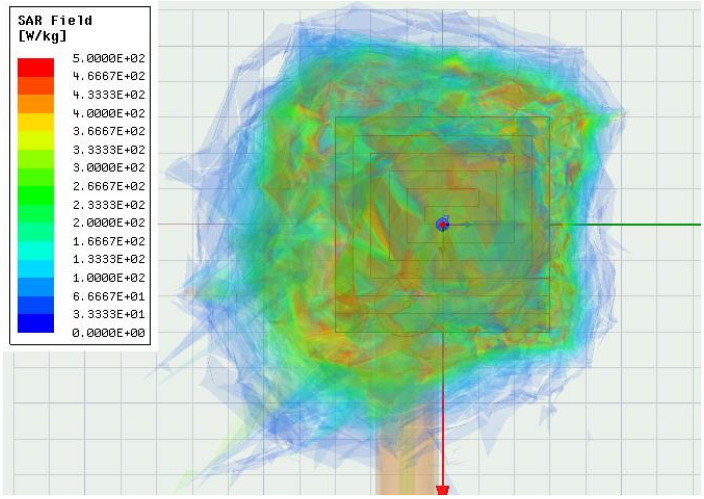

Figure 39.a Simulated SAR distribution when power 50 dBm

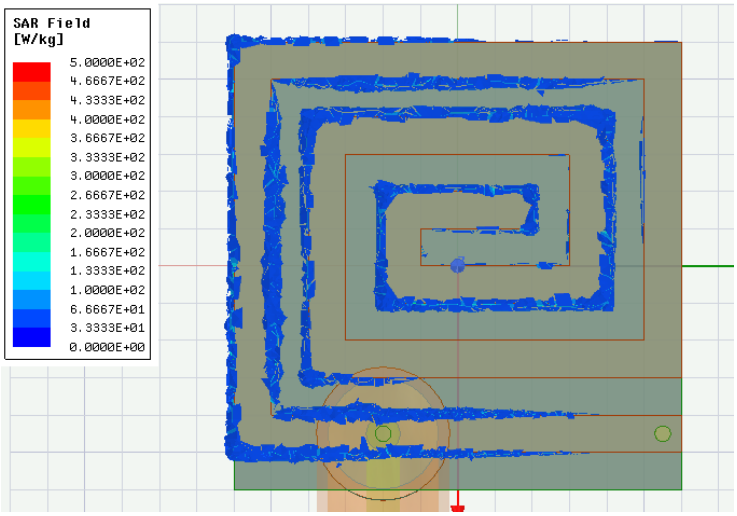

Figure 39.b Simulated SAR distribution when power 6 dBm

CHAPTER 8

CONCLUSION

8.1 Results and Discussion

In this project the development and simulation of an implantable antenna taking action against microwave hyperthermia operating at the frequency of 2.45 GHz have been described. The project started with a simple antenna design. Thanks to this simple antenna design, I learned to use the HFSS software. Some parametric analysis was done and the effect of changes of these parameters on the resonant frequency of the cavity backed slot antenna was observed. For example, doing this I made the conclusion that slot length is the most critical parameter for determining the resonant frequency of cavity backed slot antenna. Afterwards, the same analysis is done to the cavity backed slot antenna in human fat tissue. The effect of medium on the antenna characteristics is observed. Changing antenna parameters, the return loss of -20 dB is achieved. The bandwidth of the antenna is also increased.

After electromagnetics analysis the thermal analysis is done, and I learned to use software ANSYS Workbench during my project. But the thermal demonstration of cavity backed slot antenna was not satisfactory, only an increase of 0.13 °C is observed. The main reason for this was the distribution of the SAR. The region was so small.
Although the result of cavity backed slot antenna was not satisfactory, the design and simulation of cavity backed slot antenna electrically and mechanically helped me a lot practicing the applications HFSS and Workbench.

It would be nice to have a reference for my thermal analysis. Because I am not sure if my thermal analysis setup is successful or not. I may have made a mistake when applying heat transfer between surfaces. To clarify this question, it would be good to model an antenna, which has developed and reported in literature. For this purpose, I modeled the coaxial-slot antenna, developed by Koichi Ito and Kazuyuki Saito.

The performance of the coaxial-slot antenna is not judged by its return loss and radiation pattern, but by its specific absorption rate (SAR) and the temperature distribution. It is observed that the SAR values of the modelled antenna satisfactory. The simulated SAR values and temperature distributions are compared with the measured results reported in the paper, and my thermal analysis setup is verified. Besides this antenna gives the idea to design an antenna which have large SAR values in its neighborhood. One should design an antenna whose structure resembles the already designed coaxial slot antenna.

After meetings with my principal investigator and some literature review, I decided to use C type slotted antenna. After optimizing its performance and analyzing mechanically I observe that the C-type antenna has a better performance in terms of heating. But the temperature is still below 40 °C, which was the performance evaluation criteria.

The heating strongly depends on the antenna type. More antenna types should be reviewed and tested later in my project.

I would love to emphasize the fact that it is really hard to simulate an exact medium and observe the heating in that medium. For instance, the C type antenna is simulated inside human bone. But the real human bone consists of different parts and materials. Its thermal and dielectric properties strongly depend on ambient conditions and it is not homogenic as it is assumed in simulations. The software I used for heating

simulations was Ansys Workbench, which is a software environment for performing structural, thermal and electromagnetic analyses. It was a little bit hard for me learning how to use this software for biomedical purposes, because the documentation on the internet was restricted.

8.2 Social, Environmental and Economic Impact

Although from an economical point of view, the project does not aim for any profit or further labor, if the project will turn out to be a real success at the end of EE 492, then it will yield a great economic and social benefits for users and device manufacturers. Moreover, using the designed antenna will save the patients and physicians a lot of time, because the implant antenna has its own feedback mechanism. Implicitly it will reduce the cost associated with the healthcare and it will improve the healthcare provided. It is a fact that implanted wireless devices are going to find wider application in tomorrow's world. Whether my project will be completed successfully is not going to change this fact.

8.3 Cost Analysis

The project required a workstation on which the simulations to be implemented. I used the workstation of BOUNTENNA during my project. To create the measurement setup a vector network analyzer (VNA), a rotary stage and absorbers will be used (in EE 492). Moreover, I invested a specified amount of time for this project throughout the year.

8.4 Standards

In this project, the engineering ethics and code of conduct is considered. Besides, the IEEE, IET, ETSI and EU standards will be followed in addition to Turkish standards.

APPENDIX

APPENDIX A

```
clc,

clf;









fid1_1   = fopen('water1.dat','rt');  %enter your water txt
SS1_1    = textscan(fid1_1, '%f %f %f');

fid1_2   = fopen('water2.dat','rt');
SS1_2    = textscan(fid1_2, '%f %f %f');

fid1_3   = fopen('water3.dat','rt');
SS1_3    = textscan(fid1_3, '%f %f %f');


fid0_1   = fopen('air1.dat','rt');    %enter your air txt
SS0_1    = textscan(fid0_1, '%f %f %f');

fid0_2   = fopen('air2.dat','rt');
SS0_2    = textscan(fid0_2, '%f %f %f');

fid0_3   = fopen('air3.dat','rt');
SS0_3    = textscan(fid0_3, '%f %f %f');


fid_1   = fopen('fat1.dat','rt');    %enter your unkown txt
SS_1    = textscan(fid_1, '%f %f %f');

fid_2   = fopen('fat2.dat','rt');
SS_2    = textscan(fid_2, '%f %f %f ');

fid_3   = fopen('fat3.dat','rt');
SS_3    = textscan(fid_3, '%f %f %f');




number_of_rows=size(SS_1{1,1},1);


f=zeros(number_of_rows,1,'double');
real_1=zeros(number_of_rows,1,'double');
```

```
imag_1=zeros(number_of_rows,1,'double');
phase_1=zeros(number_of_rows,1,'double');
mag_1=zeros(number_of_rows,1,'double');

real1=zeros(number_of_rows,1,'double');
imag1=zeros(number_of_rows,1,'double');

real0=zeros(number_of_rows,1,'double');
imag0=zeros(number_of_rows,1,'double');

for i=1:1:number_of_rows

        f(i,1)              = SS_1{1,1}(i,1)*10^6;


        real_1(i,1)         = (SS_1{1,2}(i,1)+SS_2{1,2}(i,1)+SS_3{1,2}(i,1))/3;
        imag_1(i,1)         = (SS_1{1,3}(i,1)+SS_2{1,3}(i,1)+SS_3{1,3}(i,1))/3;
        phase_1(i,1)        = atan(imag_1(i,1)/real_1(i,1));
        mag_1(i,1)          = sqrt(real_1(i,1)^2+imag_1(i,1)^2);

        real1(i,1)          = (SS1_1{1,2}(i,1)+SS1_2{1,2}(i,1)+SS1_3{1,2}(i,1))/3;
        imag1(i,1)          = (SS1_1{1,3}(i,1)+SS1_2{1,3}(i,1)+SS1_3{1,3}(i,1))/3;


        real0(i,1)          = (SS0_1{1,2}(i,1)+SS0_2{1,2}(i,1)+SS0_3{1,2}(i,1))/3;
        imag0(i,1)          = (SS0_1{1,3}(i,1)+SS0_2{1,3}(i,1)+SS0_3{1,3}(i,1))/3;


end
```

```
patlayan_eps=0;
patlayan_cond =0;
Y=0;



c = 3*10^8;
```

```
Eps_t        =  2.03-0.004j;

C_1 = zeros(number_of_rows,3,'double');

condvector_1 = zeros(1,number_of_rows,'double');
epsreal_1 = zeros(1,number_of_rows,'double');

patladi=0;

    for i=1:1:number_of_rows

        it=0;

        w            =  f(i,1)*2*pi;
        Eps_1        =  4.6+(78.3-4.6)/(1+(1j*w*8.08*10^(-12))^(1-0.014));


        wavelength_t =  (c/(sqrt(real(Eps_t))))/f(i,1);
        Beta_t       =  2*pi/wavelength_t;
        Beta_0       =  (2*pi*f(i,1))/c;

        R_m          =  real_1(i,1) + imag_1(i,1)*(1j);

        R_m0         =  real0(i,1) + imag0(i,1)*(1j);
        R_m1         =  real1(i,1) + imag1(i,1)*(1j);
        p_R1         = (Eps_t^(1/2)-Eps_1^(1/2))/(Eps_t^(1/2)+Eps_1^(1/2)) ;

        p_R0         = (Eps_t^(1/2)-1)/(Eps_t^(1/2)+1) ;

        L_f          =  10000;
        L_0          =  500;

        D_0 = (log(R_m0)+log((1+ p_R0*exp((-2j)*Beta_0*L_0)/(p_R0+exp((-
2j)*Beta_0*L_0))))/((-2)*1j)/Beta_t;



            while (1)
            L_0 = (c/(w*Eps_1^(1/2)))*atan((((-1j)*Eps_t^(1/2))/Eps_1^(1/2))*(1-
(R_m1*exp((2j)*Beta_t*D_0)))/(1+(R_m1*exp((2j)*Beta_t*D_0))));

            if (abs(L_f - L_0)<=0.0000000001 )
                break
            end
            L_f = L_0;
            D_f = (     log((R_m0)*(1+ p_R0*exp((-2j)*Beta_0*L_f))/(p_R0+exp((-
2j)*Beta_0*L_f)))           )/((-2j)*Beta_t);


            D_0 = D_f;
            it=it+1;
            if (it>99)
                patladi=4
                i
                break
```

```
            end

            end
it=0;
            Ro = R_m*exp((2j)*D_0*Beta_t);
            Eps_0 = (sqrt(Eps_t)*c*(1-Ro))    /    (w*L_f*(1+Ro)*(1j));


        while(1)

            X = w*L_f*sqrt(Eps_0)    /    c;

            Eps_f = (sqrt(Eps_t)/(1j))   *   (c/(w*L_f))    *    ((1-Ro)/(1+Ro))   *   X
*   cot(X);

            if (abs(real(Eps_0) - real(Eps_f))<=0.0000000001)
                if (abs(imag(Eps_0) - imag(Eps_f))<=0.0000000001)
                    break
                end
            end

            it=it+1;

            if (it>99)
                patladi=5
                i
                break
            end

         Eps_0 = Eps_f;

         end
         Eps_0 = Eps_f;
         cond=imag(-Eps_0)*w*8.85*10^(-12);



        condvector_1(i) = cond;
        epsreal_1(i) = real(Eps_0);

      C_1(i,1) = w/(2*pi);
      C_1(i,2) = cond;
      C_1(i,3) = real(Eps_0);


    end


y = smoothdata(epsreal_1,'movmean','SmoothingFactor',0.6);
y = smoothdata(y,'movmean','SmoothingFactor',0.5);
y = smoothdata(y,'movmean','SmoothingFactor',0.4);
y = smoothdata(y,'movmean','SmoothingFactor',0.3);
y = smoothdata(y,'movmean','SmoothingFactor',0.2);
y = smoothdata(y,'movmean','SmoothingFactor',0.1);
```

```
y = smoothdata(y,'movmean','SmoothingFactor',0.05);
y = smoothdata(y,'movmean','SmoothingFactor',0.05);
y = smoothdata(y,'movmean','SmoothingFactor',0.05);
y = smoothdata(y,'movmean','SmoothingFactor',0.05);
y = smoothdata(y,'movmean','SmoothingFactor',0.05);
y = smoothdata(y,'movmean','SmoothingFactor',0.05);
y = smoothdata(y,'movmean','SmoothingFactor',0.05);
y = smoothdata(y,'movmean','SmoothingFactor',0.05);
y = smoothdata(y,'movmean','SmoothingFactor',0.05);
y = smoothdata(y,'movmean','SmoothingFactor',0.05);
y = smoothdata(y,'movmean','SmoothingFactor',0.05);
y = smoothdata(y,'movmean','SmoothingFactor',0.05);
y = smoothdata(y,'movmean','SmoothingFactor',0.05);
y = smoothdata(y,'movmean','SmoothingFactor',0.05);
y = smoothdata(y,'movmean','SmoothingFactor',0.05);
y = smoothdata(y,'movmean','SmoothingFactor',0.05);





   subplot(2,2,1)
   plot(f,y)
   title ("Smoothed")
   subplot(2,2,2)
   plot(f,epsreal_1)
   title ("Calculated")

   y = smoothdata(condvector_1,'movmean','SmoothingFactor',0.6);
y = smoothdata(y,'movmean','SmoothingFactor',0.5);
y = smoothdata(y,'movmean','SmoothingFactor',0.4);
y = smoothdata(y,'movmean','SmoothingFactor',0.3);
y = smoothdata(y,'movmean','SmoothingFactor',0.2);
y = smoothdata(y,'movmean','SmoothingFactor',0.1);
y = smoothdata(y,'movmean','SmoothingFactor',0.05);
y = smoothdata(y,'movmean','SmoothingFactor',0.05);
y = smoothdata(y,'movmean','SmoothingFactor',0.05);
y = smoothdata(y,'movmean','SmoothingFactor',0.05);
y = smoothdata(y,'movmean','SmoothingFactor',0.05);
y = smoothdata(y,'movmean','SmoothingFactor',0.05);
y = smoothdata(y,'movmean','SmoothingFactor',0.05);
y = smoothdata(y,'movmean','SmoothingFactor',0.05);
y = smoothdata(y,'movmean','SmoothingFactor',0.05);
y = smoothdata(y,'movmean','SmoothingFactor',0.05);
y = smoothdata(y,'movmean','SmoothingFactor',0.05);
y = smoothdata(y,'movmean','SmoothingFactor',0.05);
y = smoothdata(y,'movmean','SmoothingFactor',0.05);
y = smoothdata(y,'movmean','SmoothingFactor',0.05);
y = smoothdata(y,'movmean','SmoothingFactor',0.05);

   subplot(2,2,3)
   plot(f,y)
   title ("Smoothed")
   subplot(2,2,4)
```

```
    plot(f,condvector_1)
    title ("Calculated")



fclose(fid1_1);
fclose(fid1_2);
fclose(fid1_3);
fclose(fid0_1);
fclose(fid0_2);
fclose(fid0_3);
fclose(fid_1);
fclose(fid_2);
fclose(fid_3);
```

BIBLIOGRAPHY

BIBLIOGRAPHY

[1] OECD (2017), "Hip and knee replacement", in Health at a Glance 2017: OECD Indicators, OECD Publishing, Paris.

[2] Third AJRR Annual Report on Hip and Knee Arthroplasty Data. (2016). [ebook] Rosemont, Illinois: American Joint Replacement Registry, pp.13-21. Available at: http://www.ajrr.net/images/annual_reports/AJRR_2016_Annual_Report_final.pdf [Accessed 21 Feb. 2019].

[3] Vanhegan, I. S., Malik, A. K., Jayakumar, P., Islam, S., Haddad, F. S. 2012. "A financial analysis of revision hip arthroplasty: the economic burden in relation to the national tariff", J Bone Joint Surg Br, 94(5), 619-623.

[4] The NJR Editorial Board, Ed., "National Joint Registry 13th Annual Report 2016," rep., 2016.

[5] L. Montanaro, P. Speziale, D. Campoccia, S. Ravaioli, I. Cangini, G. Pietrocola, S. Giannini, and C. R. Arciola, "Scenery of Staphylococcus implant infections in orthopedics," Nov-2011. [Online]. Available: https://www.futuremedicine.com/doi/pdf/10.2217/fmb.11.117. [Accessed: 20-Feb-2019].

[6] G. D. Ehrlich, F. Z. Hu, Q. Lin, J. W. Costerton, and J. C. Post, "Intelligent implants to battle biofilms | Request PDF," 03-Nov-2004. [Online]. Available: https://www.researchgate.net/publication/292688877_Intelligent_implants_to_battle_biofilms. [Accessed: 20-Feb-2019].

[7] S. Dumanli, "A cornered shallow cavity backed slot antenna suitable for smart hip implants," *2016 10th European Conference on Antennas and Propagation (EuCAP)*, 2016.

[8] H. Qi, K. Xiao, F. Zhao, S. Chai, and W. Yin, "A Design of Wide Band and Wide Beam Cavity-Backed Slot Antenna Array with Slant Polarization," *International Journal of Antennas and Propagation*, 23-Oct-2016. [Online]. Available: https://www.hindawi.com/journals/ijap/2016/8980495/. [Accessed: 07-Mar-2019].

[9] Ilka Dove, "Analysis of Radio Propagation Inside the Human Body for in ...," Aug-2014. [Online]. Available: http://essay.utwente.nl/66071/1/Dove_MA_TE.pdf. [Accessed: 10-Mar-2019].

[10] Itis.swiss. (2019). *DATABASE » IT'IS Foundation*. [online] Available at: https://itis.swiss/virtual-population/tissue-properties/database/ [Accessed 11 Mar. 2019].

[11] *Thermo-Dielectric Breast Phantom for Experimental Studies of Microwave Hyperthermia - IEEE Journals & Magazine*. [online] Available at: https://ieeexplore.ieee.org/stamp/stamp.jsp?tp=&arnumber=7152875&tag=1 [Accessed 5 Dec. 2019].